Aus der Universitätsklinik

für Anästhesiologie und Intensivmedizin

Ärztlicher Direktor: Professor Dr. K. Unertl

Role of vasodilator-stimulated phosphoprotein (VASP) in myocardial ischemia-reperfusion injury

Inaugural-Dissertation
zur Erlangung des Doktorgrades
der Medizin

der Medizinischen Fakultät
der Eberhard Karls Universität
zu Tübingen

Vorgelegt von

Sarah Bender

aus

Stuttgart

- 2011 -

Dekan: Professor Dr. I. B. Autenrieth
1. Berichterstatter: Professor Dr. P. Rosenberger
2. Berichterstatter: Professor Dr. T. Schroeder

Table of contents

List of Figures

Abstract

Recent work has suggested neutrophils to facilitate the movement of platelets across cellular barriers and the formation of platelet-neutrophil complexes (PNCs) to aggravate the severity of inflammatory tissue injury. Given the importance of vasodilator stimulated phosphoprotein (VASP) for the control of platelet activation we pursued the role of VASP on the formation of PNCs in a model of myocardial ischemia-reperfusion (IR) injury. Initial *in-vitro* studies revealed neutrophils to facilitate transendothelial movement of platelets and that the exposure to shear stress results in increased PNC formation. Phosphorylation of VASP at Ser-157 or Ser-239 significantly reduced neutrophil facilitated transendothelial movement of platelets. Following IR injury *VASP*$^{-/-}$ animals demonstrated reduced presence of PNCs within ischemic tissue which was associated with reduced myocardial IR injury. Further studies employing chimeric animals and platelet crossover injection identified VASP expression within platelets to be of great importance for the formation of PNCs. Studies in WT, *VASP*$^{-/-}$ and chimeric animals identified the phosphorylation of hematopoietic VASP at Ser-153 or Ser-235 to reduce the formation of PNCs and dampen the extent of myocardial IR injury. Previously unappreciated, VASP holds a key function for the formation of PNCs which is crucially important for the extent of myocardial IR injury.

Zusammenfassung

Neueste Studien konnten zeigen, dass neutrophile Granulozyten die Migration von Thrombozyten durch geschlossene Zellbarrieren erleichtern. Die Bildung von Thrombozyten-Neutrophilen-Komplexen (PNC) erhöht laut diesen Studien den Schweregrad einer inflammatorischen Schädigung des betroffenen Gewebes. Da Vasodilator Stimulated Phosphoprotein (VASP) bekanntermaßen die Thrombozyten-Aktivierung beeinflusst, untersuchten wir die Rolle von VASP auf die Bildung von PNCs in einem myokardialen Ischämie-Reperfusions-(IR)-Schädigungsmodell.

Durch *in-vitro* Studien konnten wir belegen, dass die transendotheliale Translokation von Thrombozyten durch neutrophile Granulozyten beeinflusst wird und erhöhte Scherkräfte zu einer vermehrten PNC Bildung führen. Kam es zu einer Phosphorylierung von VASP an den Aminosäuren Ser-157 oder Ser-239 (bzw. Ser-153 oder Ser-235 im Tiermodell), so wurde diese Translokation der Thrombozyten signifikant reduziert. VASP Knockout-Tiere wiesen im Vergleich zu WT-Tieren nach IR-Schädigung eine wesentlich geringere Konzentration von PNCs im ischämischen Gewebe auf. In der Folge kam es bei den VASP Knockout-Tieren auch zu einer geringeren Ausprägung des Reperfusionsschadens. Überkreuzinjektionen von Thrombozyten in knochenmarkchimäre Tiere zeigten auf, dass vor allem die VASP-Expression in den Thrombozyten für die Bildung der PNCs von zentraler Bedeutung ist.
Experimente mit WT, *VASP*$^{-/-}$ und chimären Tieren konnten ferner zeigen, dass die Phosphorylierung von hämatopoetischem VASP an Ser-153 oder Ser-235 zu einer Reduktion der PNCs und einer Minimierung der myokardialen IR-Schädigung führte. Auf diese Weise konnten wir belegen, dass VASP eine Schlüsselrolle bei der Bildung von PNCs spielt und somit das Ausmaß einer myokardialen IR-Schädigung entscheidend beeinflusst.

Abbreviations, Glossary

aa	Amino acid
AAR	Area at risk
Abl	Abelson murine leukemia viral oncogene
AC	Adenylate cyclase
ACS	acute coronary syndrome
ActA	actin-assembly inducing protein Listeria monocytogenes surface protein
ADP	Adenosine diphosphate
AMP	adenosine monophosphate
AMPK	AMP activated protein kinase
ANP	Atrial natriuretic peptide
Av Ena	Avian Ena
BCEC	brain capillary endothelial cells
BM	Bone marrow
cAMP	Cyclic adenosine monophosphate
CC	coiled-coil
CD11a	Cluster of Differentiation antigen 11a
CD11a/CD18	= LFA-1 = lymphocyte function-associated antigen-1
CD11b	Cluster of Differentiation antigen 11b = 170 kDa subunit of MAC-1
CD11b/CD18	= MAC-1 = Macrophage-1 antigen = integrin αMβ2
CD18	Cluster of Differentiation antigen 18 = Subunit of MAC-1
CD41	Cluster of Differentiation antigen 41 = 140kD glycoprotein expressed by platelets and megakaryocytes = IIb part of GPIIb/IIIa

CD41/CD61	= GPIIb/IIIa
CD61	Cluster of Differentiation antigen 61 = 105 kDa transmembrane glycoprotein expressed on platelets, megakaryocytes, and endothelial cells = IIIa part of GPIIb/IIIa
cGMP	Cyclic guanosine monophosphate
DAB	Diaminobenzidin
Ena	Drosophila melanogaster Enabled
EVH 1/2	Ena-VASP homology domain 1/2
EVL	Ena-VASP-like
FAB	filamentous actin-binding site
FACS	Fluorescence activated cell sorting
GAB	globular actin-binding site
GC-A	guanylyl cyclase A receptor
GMP	guanosine monophosphate
GP IIb/IIIa	Glycoprotein IIb/IIIa = integrin αIIbβ3 = CD41/CD61= fibrinogen-receptor
GP5	GPPPPP; G = Glycine, P = Prolin
GPIbα	glycoprotein Ibα
Gy	Gray, SI unit of absorbed radiation
HIF-1	hypoxia inducible factor 1
HMEC	human microvascular endothelial cells
ICAM-2	intercellular adhesion molecule-2
IR	ischemia-reperfusion
IRSP53	Insulin receptor substrate protein of 53 kDa
JAM-1	junctional adhesion molecule-1
LCA	left coronary artery
LFA-1	lymphocyte function-associated antigen-1 = CD11a/CD18

MAC-1	= Macrophage-1 antigen = integrin αMβ2 = CD11b/CD18 = complement receptor
Mena	Mammalian Ena
MPO	myeloperoxidase assay
NIH	National Institutes of Health
NO	Nitric oxide
NOS	Nitric oxide synthase
$P2Y_{12}$	purinergic receptor 12, G-protein coupled
PAC-1	procaspase activating compound 1 = GPIIb/IIIa epitope
PAOD	peripheral artery occlusive disease
PBS	phosphate buffered saline
PGE1	Prostaglandin E_1
PKA	protein kinase A
PKC	protein kinase C
PKG	protein kinase G
PMA	Phorbol 12-myristate 13-acetate
PMNs	polymorph nuclear neutrophils
PNC	Platelet-neutrophil complex
PP	protein phosphatase
PRI	Platelet Reactivity Index
Pro	Prolin
PRR	proline rich region
PSGL-1	P-selectin glycoprotein ligand-1
RIPA buffer	radio immunoprecipitation assay buffer = cell lysis buffer
SEM	Structural equation modeling
Ser-157	VASP phosphorylation site at Serine 157
Ser-239	VASP phosphorylation site at Serine 239
sGC	soluble guanylyl cyclase

SH3	Src Homology 3
siRNA	Small interfering Ribonucleic acid
siVASP	siRNA silencing VASP
SOC	store operated cation channel
SPCN	spectrin non-erythroid (brain) alpha chain, synonym for αII-spectrin
Src	Sarcoma
TD	tetramerization domain
Thr-278	VASP phosphorylation site at Threonin 278
TRPC4	Transient receptor potential cation channel, subfamily C, member 4
TTC	triphenyltetrazolium chloride
UNC-34	Uncoordinated family member
VASP	Vasodilator stimulated Phosphoprotein
VASP-P	Phosphorylated VASP
WT	Wild type
WW	short form for Tryptophan-Tryptophan region
ZO-1	Zonula occludens-1 protein
αIIbβ3	= Glycoprotein IIb/IIIa = integrin αIIbβ3 = CD41/CD61 = fibrinogen-receptor

1 Introduction

1.1 VASP

Vasodilator stimulated Phosphoprotein (VASP) was primarily described by Halbrugge and Walter (1989) in platelets and endothelial cells during aggregation processes.[1] It is known today as an omnipresent cytoskeletal protein found in nearly every cell throughout the human body and within many other organisms, e.g. in vascular endothelial cells, smooth muscle cells, platelets, fibroblasts, mesangial cells and brain capillary endothelial cells.[1-5] VASP is known to play an important role in actin reliant procedures like cell stability, filament elongation, focal adhesion and cell to cell contact, and as such it is not surprising that it also holds an important role in the maintenance of barrier function.[6] Dysfunctional barriers facilitate trespassing of harmful particles (e.g. bacteria) which, in case of a deficient immune system, can be the cause of severe illness. Protein kinase A (PKA) and Protein kinase C (PKC) pathway activation during inflammation partly regulates the degree of endothelial permeability via VASP phosphorylation.[7-12]

Furthermore VASP has a central impact on the development of haemapoetic cells and platelet aggregation. A knock-out of VASP leads to modified expression of megakaryocytes, also known as precursor cells of platelets in bone marrow. Platelets play an important role in homeostasis and stabilize barrier function. Activated platelets release granula: e.g. adenosindiphosphate (ADP) activating fibrinogen receptor GP IIb/IIIa (also known as integrin α_{IIb} β_3) which results in fibrinogen cross linking of platelets, serotonin and thromboxane release causing vasoconstriction and further platelet activation (Figure 1).[13-17] Thienopyridines repress the described platelet adhesion process by selectively and irreversibly binding to ADP receptor $P2Y_{12}$. That is the reason why well-known thienopyridines like Prasugrel, Ticlopidine and Clopidogrel are therapeutically used as anti-platelet agent to reduce the incidence of thrombotic complications e.g. in patients after stent-implantation, with PAOD (peripheral artery occlusive disease) or ACS (acute coronary syndrome).[13,17-20] As a measure of platelet activation the PRI-VASP method

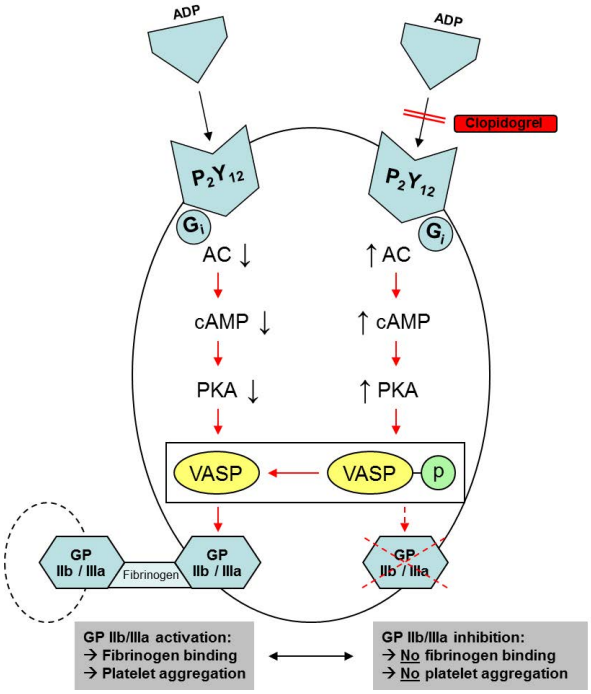

Figure 1 – Role of VASP in platelet aggregation.[13-17]

ADP = Adenosindiphosphat, $P2Y_{12}$ = G-Protein (Gi) coupled adenosine receptor, AC= Adenylyl cyclase, PKA = protein kinase A, VASP = vasodilator stimulated phosphoprotein; VASP-P = phosphorylated VASP, GPIIb/IIIa = fibrinogen receptor

(**P**latelet **R**eactivity **I**ndex) is used today in clinical routine. This method detects the phosphorylation status of VASP at Ser-239 in patients during Clopidogrel treatment and thereby predicts non-responders.[21-22] The treatment can in consequence be changed before thrombotic incidents in high risk occur.[16]

VASP is a member of the Ena/VASP family, a group of various structural similar proteins known for their influence on different actin-reliant processes like cell motility, vesicle movement, cell–matrix and cell–cell adhesion, cell migration and axon guidance.[23] Their amino acid sequences contain three highly conserved domains: a proline rich region (PRR) bordered by two Ena-VASP homology domains (EVH1, EVH2).[23]

In Mammalians the Ena/VASP family includes: Mammalian Ena (Mena), Vasodilator-stimulated Phosphoprotein (VASP) and Ena-VASP-like (EVL).[7] Various species have been identified to contain homologues of the Ena/VASP

family and have been subject of numerous scientific investigations. Figure 2 gives an overview of most commonly cited representatives.[24]

Vertebrate homologues	Other homologues
Mammalians[7]: e.g. *Bos Taurus*, *Canis lupus familiaris*, apes (avEna), *Rattus norvegicus, Pongo abelii.* **Birds:** e.g. *Gallus gallus* (Avian Ena = avEna) **Amphibia:** e.g. *Xenopus Ena* (XEna).[25] **Fish:** e.g. *Danio rerio.*	**Insects:** e.g. *Drosophila melanogaster*[23], *Gryllus bimaculatus.* **Nematodes:** e.g. *Caenorhabditis elegans* (UNC-34).[23] **Mycetozoa:** e.g. *Dictyostelium discoideum.*[23] **Bacteria:** *Listeria monocytogenes.*

Figure 2 – Origin and homologues of Ena/VASP family.[24]

1.2 Structure of VASP

VASP is represented on chromosome 19q13.2-q13.3 (human) and chromosome 7 A3 (mice) on an approximately 20 kb long DNA region. Its gene consists of 13 exons.[26] Its amino acid (aa) sequence in human (380 amino acids) is 89% identical compared to mice (376 amino acids).[26]

The knockout of Mena, VASP and EVL (mmvvee) in mice at the same time is inconsistent with their survival: late stage embryonic lethality is caused by actin cytoskeleton remodeling failures leading to deficient structural stability, edema and internal bleeding.[27]

The Protein can be structurally and functionally sub-divided into three main regions (Figure 3):

- Ena-VASP homology domain 1 (EVH1) on the N-terminal part of the protein,
- a central proline rich region (PRR) and
- a C-terminal Ena-VASP homology domain (EVH2).[6]

To simplify further explanations of VASP-structure, only the human representative of VASP will be described.

In the human VASP-protein the amino acids 1-114 form EVH1. Its affinity to “FPPPP” sequences adducts proteins important for cell morphology, motility and actin remodelling (Figure 4).[28-29] The central proline-rich region (PRR)

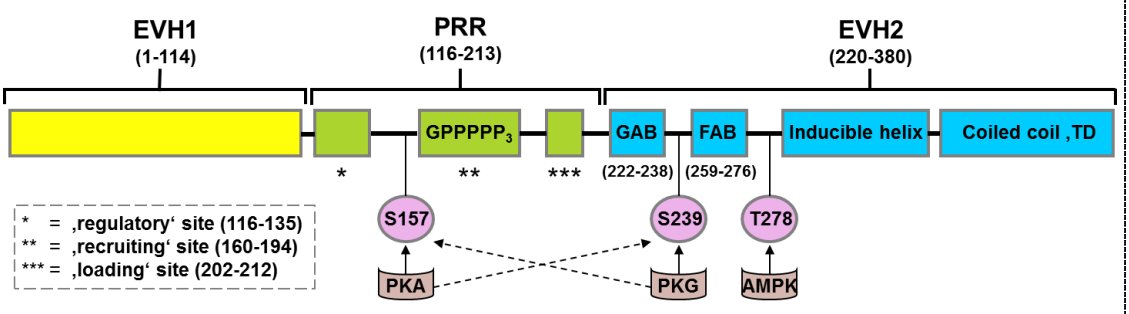

Figure 3 – Human VASP structure and phosphorylation sites.[6,30-35]
EVH = Ena-VASP homology domain, PRR= proline rich region, GAB/FAB = globular / filamentous actin-binding site, TD = Tetramerization domain, S157/S239/T278 = phosphorylation sites at serine 157, serine 239 and threonin 278; PKA = protein kinase A, PKG = protein kinase G, AMPK = AMP activated protein kinase.

includes a regulatory site (116–135 aa), featuring proteins with SH3 (Src Homology 3) and WW (Tryptophan-Tryptophan) domains like Abl, Src, Alpha-II-spectrin (SPCN) and IRSP53 to link. Furthermore PRR includes a recruiting poly-Pro site (160–194aa) with four copies of a GPPPPP (GP5) motif with the ability to attract and bind several profilin-actin compounds and a loading site (201–211aa) in charge of transporting the recruited complexes to the GAB domain (Figure 3).[28-29] On the C-terminal end of VASP EVH2 can be found. It comprehends a globular actin-binding site (GAB), a filamentous actin-binding site (FAB), an inducible helix and a coiled-coil (CC) tetramerization domain (TD; 336-380aa). In summary, EVH2 is thought to determine tetramerization and

Protein	Function
Vinculin	cytoskeletal protein involved in focal adhesion[36]
Lamellipodin	colocalizes with VASP at the tips of lamellipodia / filopodia[37]
Zyxin	zinc-binding phosphoprotein, concentrated at focal adhesions and along the actin cytoskeleton[38]
ActA	Listeria monocytogenes surface protein[39]
Fyb/SLAP	adapter proteins leading Ena/VASP to T-cell receptor, localization: lamellipodia of spreading platelets)[40]
Migfilin	component of cell-matrix adhesions, biphasic regulator of cell migration[41]
Palladin	actin-associated protein containing proline-rich motifs[6,42]

Figure 4 – EVH1 binding proteins.[24]

actin binding and was shown to be responsible for capturing barbed ends and executing anti-capping activity.[31-33]

1.3 VASP Phosphorylation

Human VASP has a molecular mass of 46 kDa in an unphosphorylated state and shifts to 50 kDa when phosphoylated at Ser-157. VASP has three phosphorylation sites: Ser-157, Ser-239 and Thr-278 (Ser-153, Ser-235 and Thr-274 in mice, respectively) (Figure 3). These sites are phosphorylated with different affinity by cAMP-, cGMP-dependent protein kinases (PKA, PKG) and AMP-activated protein kinase (AMPK). Ser-157 is preferentially phosphoylated by PKA, whereas Ser-239 is predominantly a substrate of PKG. Thr-278 was lately found to be substrate of AMPK. Prostaglandin E1 (PGE1) results in a VASP phosphorylation at Ser-157, through rising cAMP levels triggering PKA activation. ANP is an upstream regulator of VASP phosphorylation at Ser-239: it increases PKG activity by heightening intracellular cGMP levels via the GC-A (guanylyl cyclase A) receptor.[43] Dephosphorylation is regulated by different protein phosphatases (PP): PP-1, PP2A, PP2B and PP2C.[44-46]

VASP phosphorylation is also affected through nitric oxide (NO). NO-Synthase (NOS) catalyses the formation of nitric oxide out of L-arginine. This process is triggered by shear stress and rising VEGF levels. NO stimulates soluble guanylyl cyclase (sGC), which increases intracellular cGMP levels and leads to activation of PKG. As a consequence VASP is phosphorylated mainly at Ser-239 whereas intracellular Ca^{2+} levels decrease. The latter being potentially caused by an association of the phosphorylated VASP with TRPC4 (Transient receptor potential cation channel, subfamily C, member 4) in the plasma membrane, which results in an inhibition of store operated Ca^{2+} entry (SOC). VASP phosphorylation at Ser-239 consequently leads to smooth muscle relaxation.[3,47-51]

Another pathway which influences VASP phosphorylation significantly is the PKA-pathway. Prostacyclin (PGI2), a cyclooxygenase product derived from arachidonic acid, can be seen as an upstream regulator of PKA. Its binding to

prostacyclin receptor activates G_s protein, which, in turn, augments adenylyl cyclase activity leading to rising intracellular cAMP levels. This however induces PKA to phosphorylate VASP at Ser-157.[52] A famous prostacyclin analogue already used today in daily clinical practice is ilioprost (ILO), known for its efficiency in treatment of pulmonary arterial hypertension (PAH) and thromboangiitis obliterans.[53-55]

1.4 VASP in myocardial ischemia-reperfusion injury and transmigration

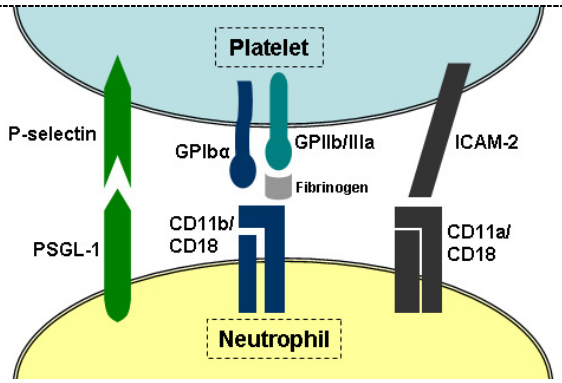

Figure 5 – Neutrophil-Platelet interaction.
modified after Landolfi and Zarbock.[14,56] ICAM-2 = intercellular adhesion molecule-2; CD11a/CD18 = LFA-1 = Lymphocyte function-associated antigen 1 ; CD11b/CD18 = MAC-1 = Macrophage-1 antigen; PSGL-1 = P-selectin glycoprotein ligand-1; GPIbα = glycoprotein Ibα ; GPIIb/IIIa = integrin αIIbβ3 = CD41/CD61 = fibrinogen-receptor

Myocardial ischemia-reperfusion (IR) injury is amongst the leading health problems worldwide.[57] The importance of neutrophils for myocardial IR injury is supported by the fact that depletion or inhibition of neutrophils results in reduced IR organ injury. Furthermore a positive correlation of the number of neutrophils and the extent of reperfusion injury has been well established.[58-59] Platelets are not 'innocent' bystanders during this process but aggravate myocardial tissue damage through the release of various products such as intracellular interleukins, peroxidases and other pro-inflammatory compounds.[60-61] As such the inflammatory response during reperfusion has significant impact on apoptosis within the myocardium.[62] The transmigration process can be

simplified to a three step process: leukocyte rolling, adhesion and transmigration. The first step is predominantly mediated by selectins: communicated e.g. by exposed P-selectin localized on inflamed endothelial cells or activated platelets, leukocytes attach via PSGL-1 (P-selectin glycoprotein ligand-1).[14,56,63-65] This interaction enables leukocytes to slow down under the condition of shear stress applied to them by normal blood flow. Afterwards the leukocytes are activated by chemokines and finally firmly adhere mediated by various integrins. Platelet-neutrophil complexes (PNCs) are stabilized by binding of LFA-1 (Lymphocyte function-associated antigen 1) to ICAM-2 (intercellular adhesion molecule-2) or binding of MAC-1 (CD11b/CD18, Macrophage-1 antigen) to GPIbα or GPIIb/IIIa via bridging proteins such as fibrinogen (Figure 5). Integrins then also trigger the transcellular or paracellular transmigration process. Recent work has demonstrated that the formation of platelet-neutrophil complexes (PNCs) significantly affects the extent of inflammatory tissue damage during acute lung injury and colitis.[66-67] A prerequisite for the firm adhesion between neutrophils and platelets is the fibrin mediated link of CD11b/CD18 on neutrophils and the GPIIb/IIIa receptor on platelets.[14,68-69] Bennett et al. demonstrated the importance of the cytoskeleton for the affinity of the GPIIb/IIIa receptor to bind fibrinogen.[70] A key regulatory protein for rapid dynamic changes of the cytoskeleton is VASP. VASP influences the presence of the CD11b receptor on neutrophils and is involved in the expression of the counterligand for the CD11b/CD18 receptor complex, GPIIb/IIIa.[69,71] VASP phosphorylation results in conformal changes of the cellular surface and as such might influence the exposure of surface receptors to the cellular environment.[6,31-35,72]

1.5 Scientific hypothesis

The formation of Platelet-neutrophil complexes (PNC) aggravates inflammatory processes and increases inflammatory tissue damage.[14,56,63-65] Given the importance of PNCs for the extent of inflammatory organ injury and the fact that VASP might affect the formation of PNCs, we pursued the role of VASP on the formation of PNCs during myocardial IR.

To elucidate the subject, we formulated the following central questions for this thesis:

1. Does VASP have any influence on PNCs translocation across endothelial cell layers during *in-vitro* experiments?
2. Does the knockout of VASP in mice have an impact on the degree of myocardial IR injury?
3. If yes, is this associated with a reduced presence of PNCs in the effected tissue?
4. Which compound has a bigger influence on PNC-formation in mice: myeloid VASP or tissue-bound VASP?
5. Does VASP phosphorylation affect the formation of PNCs and as such the extent of myocardial IR injury?

2 Materials and Methods

2.1 Materials

2.1.1 Commonly used material

Product name	**Product nº**	**Company**	**Provenance**
BD Plastipak Syringe BD Microlance 3	300013 302200	Becton Dickinson	Franklin Lakes, NJ, USA
Cellstar PP-test tubes 15 ml	188 271	Greiner Bio-One GmbH	Frickenhausen, Germany
Eppendorf combitips plus 2,5 ml combitips plus 0,5 ml	 0030 069.242 0030 069.420	Eppendorf AG	Hamburg, Germany
Eppendorf multipette plus	4981 000.019	Eppendorf AG	Hamburg, Germany
Eppendorf reference pipet 0,5-10µl 10-100µl 100-1000µl	 4910 000.018 4910 000.042 4910 000.069	Eppendorf AG	Hamburg, Germany
Eppendorf research pipet 500-5000µl	3111 000.173	Eppendorf AG	Hamburg, Germany
Falcon blue max 50 ml	352070	Becton Dickinson	Franklin Lakes, NJ, USA
Falcon serological pipet 1 ml 5 ml 10 ml 25 ml 50 ml	 356521 356543 356551 356525 357550	Becton Dickinson	Franklin Lakes, NJ, USA
F-bottom microplate 96 well	655101	Greiner Bio-One GmbH	Frickenhausen, Germany
Gel Cassettes 1,5 mm	NC2015	Invitrogen Corp.	Carlsbad, CA, USA

Product name	Product nº	Company	Provenance
Injekt single-use syringe 5 ml 10 ml 20 ml	 4606051V 4606108V 4606205V	B.Braun Melsungen AG	Melsungen, Germany
Latex examination gloves	PFC4303972	Ansell LTD	Bangkok, Thailand
Nunc 1,8 ml cryotube vials	368632	Nunc A/S	Roskilde, Denmark
Parafilm “M” laboratory film		Pechiney Plastic-Packaging	Chicago, IL, USA
Peha-Soft Vinyl examination gloves	PZN 8909483	PAUL HARTMANN AG	Heidenheim, Germany
Pipetboy acu	155000	Integra Bio-sciences GmbH	Fernwald, Germany
Safe-Lock tubes 0,5 ml	0030 121.023	Eppendorf AG	Hamburg, Germany
Safe-Lock tubes 1,5 ml	0030 120.086	Eppendorf AG	Hamburg, Germany
SafeSeal-tips premium 10 ml	692150	Biozym Diagnostik GmbH	Hess. Oldendorf, Germany
SafeSeal-tips premium 100 ml	692066	Biozym Diagnostik GmbH	Hess. Oldendorf, Germany
SafeSeal-tips premium 1000 ml	692079	Biozym Diagnostik GmbH	Hess. Oldendorf, Germany

2.1.2 Instrumental equipment

Product name	Company	Provenance
Adobe Photoshop CS 2	Adobe	
Analytical balance HR-200	A & D Company, Ltd.	Tokyo, Japan
Centrifuge 5417 R	Eppendorf AG	Hamburg, Germany
Diana luminescence imaging system	Raytest	Straubenhardt, Germany
Diana multifunctional darkroom	raytest GmbH	Straubenhardt, Germany

Product name	**Company**	**Provenance**
Endnote X3	Thomson Reuters	San Francisco CA USA
Gene expression macro	Bio-Rad Lab., Inc.	Munich, Germany
GENios microplate reader + Magellan software V5.03	Tecan Group Ltd.	Männedorf, Switzerland
Graph Pad Prism 5	GraphPad Software, Inc.	La Jolla, CA, USA
iCycler	Bio-Rad Lab., Inc.	Munich, Germany
Impulse sealer TISH-200	TEW Electric Heating Equipment CO., LTD	Taipei, Taiwan
Incubator	Heraeus Holding GmbH	Hanau, Germany
Kirsch super refrigerator	Glen Dimplex Deutschland GmbH	Kulmbach, Germany
Magellan software	Tecan Group Ltd.	Männedorf
Mini Trans-Blot Electrophoretic Transfer Cell	Bio-Rad Lab., Inc.	Munich, Germany
N811 KN.18 vacuum pump	KNF Neuberger	Freiburg, Germany
Novex Mini-Cell	Invitrogen	Carlsbad, CA, USA
Photometer Ultrospec 3000 pro + Thermal printer DPU-414-30B	Biochrom Ltd. Seiko Instruments Inc.	Cambridge, UK Chiba, Japan
Powerpac 3000	Bio-Rad Lab., Inc.	Hercules, CA, USA
RET basic C magnetic stirrer	IKA Works, Inc.	Wilmington, USA
Rotating plate	Infors AG	Bottmingen, Switzerland
Scotsman AF10 automatic ice machine	Frimont S.p.a.	Milano, Italy
siRNA Wizard	InvivoGen	San Diego, USA
Spreadsheet interface software		
Sterile workbench Lamin Air HB 2472	Haereus Instruments	Hanau, Germany
TD-20/20 Luminometer	Turner BioSystems, Inc.	Sunnyvale, USA
Thermocycler	Bio-Rad Lab., Inc.	Munich, Germany
Thermomixer 5436	Eppendorf AG	Hamburg, Germany
Tissue homogenizing system MICCRA D-9 + Pico DS-8/P	Art-moderne Labortechnik e.K.	Müllheim, Germany

Product name	Company	Provenance
Vortex genie 2	Scientific Industries, Inc.	Bohemia, NY, USA

2.1.3 Western Blots

Product name	Product nº	Company	Provenance
Amersham Full Range Rainbow Recombinant Protein Molecular Weight Marker	RPN 800	GE Healthcare UK Ltd	Buckingham-shire, UK
Ammonium persulfate	A9164	Sigma-Aldrich, Inc.	St.Louis, MO, USA
ANP		Sigma-Aldrich	Munich, Germany
BCA protein assay kit	23225	Thermo Fisher Scientific, Inc.	Rockford, IL, USA
Bovine Serum Albumin (BSA)	A7906-50G	Sigma	Taufkirchen, Germany
Detection buffer BCIP/NBT: ♦ 220 ml A.d. ♦ 5 ml 5M NaCl ♦ 25 ml 1M Tris-HCl ♦ BCIP ♦ NBT BioChemica	 567440 A1117 A1243	 Merck KGaA AppliChem GmbH	 Darmstadt, Germany Darmstadt, Germany
DPBS 1x (-CaCl2) (-MgCl2)	14190	Invitrogen Corp.- Gibco	Carlsbad, CA, USA
DPBS 1x (+CaCl2) (+MgCl2)	14040	Invitrogen Corp.- Gibco	Carlsbad, CA, USA
ECL detection system: ♦ 1M Tris-HCl pH 8,5 ♦ p-Coumeric-acid ♦ Luminol	 C9008 09253	 Sigma Fluka	Taufkirchen, Germany
Goat Anti-Rabbit IgG-HRP	sc-2004	Santa Cruz Biotechnology, Inc.	Santa Cruz, CA, USA
Immun-Blot-PVDF-	162-0177	Bio-Rad Lab., Inc.	Munich, Germany

Product name	Product nº	Company	Provenance
Membrane			
Loading buffer (4x), non-reducing: ♦ 1M Tris-HCl (→pH 6,8) ♦ Glycerol ♦ Sodium dodecyl sulfate ♦ Bromophenol blue	 A3452 G5516 L4390 A3640	 AppliChem GmbH Sigma-Aldrich, Inc. Sigma-Aldrich, Inc. AppliChem GmbH	 Darmstadt, Germany St.Louis, MO, USA St.Louis, MO, USA Darmstadt, Germany
Lower buffer: ♦ 1,5M Tris ♦ 0,4% Sodium dodecyl sulfate (→pH 8,8)	 A2264 L4390	 AppliChem GmbH	 Darmstadt, Germany
Magic Mark XP Western Standard	LC5602	Invitrogen	Carlsbad, CA, USA
Methanol	1.06009.2511	Merck	Darmstadt, Germany
PGE1		Sigma-Aldrich	Munich, Germany
Ponceau S solution	P7170	Sigma-Aldrich, Inc.	St.Louis, MO, USA
pVASP^{157} Rabbit mAb	3111	Cell Signaling	New England Biolabs, Frankfurt am Main, Germany
pVASP^{239} Rabbit mAb	3114	Cell Signaling	New England Biolabs, Frankfurt am Main, Germany
Ready gel cell	108BR01057	Bio-Rad Lab., Inc.	Hercules, CA, USA
Restore Western Blot Stripping Buffer	21059	Pierce	Bonn, Germany
Restore Western Blot Stripping Buffer	21059	Thermo Fisher Scientific, Inc.	Rockford, IL, USA
RIPA-buffer: ♦ EDTA	 A3145	 AppliChem GmbH	 Darmstadt, Germany

Product name	Product nº	Company	Provenance
♦ Sodium chloride ♦ Tris (→pH7.4) ♦ Igepal CA-630	567440 A2264 I8896	Merck KGaA AppliChem GmbH Sigma-Aldrich, Inc.	Darmstadt, Germany Darmstadt, Germany St.Louis, MO, USA
Rotiphorese Gel 30	3029.1	Carl Roth GmbH	Karlsruhe, Germany
SeeBlue Plus 2, Prestained Standard	LC5925	Invitrogen	Carlsbad, CA, USA
Skim milk	A0830.0500	AppliChem	Darmstadt, Germany
Speci-Mix platform mixer	M33120	Thermo Fisher Scientific, Inc.	Rockford, IL, USA
SuperSignal West Pico chemiluminescent substrate	34078	Thermo Fisher Scientific, Inc.	Rockford, IL, USA
TBS: ♦ 1000 ml A.d. ♦ 24,2 g Tris ♦ 80 g Sodium chloride ♦ Hydrochloric acid (→pH 7,6)	 A2264 567440 100319	 AppliChem GmbH Merck KGaA Merck KGaA	 Darmstadt, Germany Darmstadt, Germany
Temed	T9281	Sigma	Taufkirchen, Germany
Trans-blot cell electro-phoretic transfer cell	36S/2832	Bio-Rad Lab., Inc.	Hercules, CA, USA
Tris Glycine Buffer 10x	161-0771	Bio-Rad Lab., Inc.	Munich, Germany
Tris Glycine SDS Buffer 10x	161-0772	Bio-Rad Lab., Inc.	Munich, Germany
TWEEN 20	A4974	AppliChem GmbH	Darmstadt, Germany
Upper buffer: ♦ 0,5M Tris ♦ 0,4% Sodium dodecyl sulfate (→pH 6,8)	 A2264 L4390	 AppliChem GmbH	 Darmstadt, Germany
VASP (9A2) Rabbit mAb	3132	Cell Signaling	New England Biolabs, Frankfurt am Main, Germany
XCell SureLock	1167482-	Invitrogen Corp.	Carlsbad, CA, USA

Product name	Product nº	Company	Provenance
electrophoresis cell	625		
β-Actin (13E5) Rabbit mAb	4970	Cell Signaling	Danvers, MA, USA

2.1.4 Transmigration

Product name	Product nº	Company	Provenance
ABTS ♦ Citric buffer ♦ A.d. ♦ ABTS ♦ Hydrogen peroxide solution 30%	 A1888 1.08597	 Sigma-Aldrich, Inc. Merck KgaA	 St.Louis, MO, USA Darmstadt, Germany
ANP		Sigma-Aldrich	Munich, Germany
Butterfly winged needle infusion set	P293 A05	Hospira Inc.	Lake Forest, IL, USA
Cellstar TC tube, sterile, 12 ml	163 160	Greiner Bio-One GmbH	FrickenhausenGermany
Citric buffer: ♦ 200 mM NaCitrate ♦ 200 mM Citric Acid	 3580 8.18707	 Carl Roth GmbH Merck Schuchardt OHG	 Karlsruhe, Germany Hohenbrunn, Germany
Coulter Clenz cleaning agent	8417-222	Beckman Coulter GmbH	Krefeld, Germany
Coulter Isoton II diluent	8448011	Beckman Coulter GmbH	Krefeld, Germany
Coulter Z2	72	Coulter Electronics LTD.	Luton, England
HBSS 1x +($CaCl_2$) +($MgCl_2$) - ($CaCl_2$) - ($MgCl_2$)	 14025 14175	Invitrogen Corp. - Gibco	Carlsbad, CA, USA
Histopaque-T1077 Histopaque-T1119		Sigma-Aldrich, Inc.	St.Louis, MO, USA

Product name	Product nº	Company	Provenance
Lysis buffer ♦ EDTA solution pH.8.0 ♦ Sodium Bicarbonate ♦ Ammonium chloride	 A3145 S-8875 A0988	 AppliChem GmbH Sigma-Aldrich, Inc. AppliChem GmbH	 Darmstadt, Germany St.Louis, MO, USA Darmstadt, Germany
Megafuge 1.0R	75003060	Heraeus Instruments	Osterode, Germany
Multi-adapter for S-monovette	14.1205.050	Sarstedt AG & Co.	Nümbrecht, Germany
N-Formyl-Met-Leu-Phe (Chemotactic peptide; fMLP)	F3506	Sigma-Aldrich, Inc.	St.Louis, MO, USA
Percoll sterile ♦ 63% ♦ 72%	17-0891	GE Healthcare Bio-Sciences AB	Uppsala, Sweden
PGE1		Sigma-Aldrich	Munich, Germany
PSB 1115 potassium salt hydrate	P0373	Sigma-Aldrich, Inc.	St.Louis, MO, USA
S-monovette	02.1067.001	Sarstedt AG & Co.	Nümbrecht, Germany
Softasept N	3887138	B.Braun Melsungen AG	Melsungen, Germany
Transwell permeable supports 3,0m polyester membrane	3472	Corning Inc.	Corning, NY, USA
Triton 10% ♦ Triton X-100	 A4975	 AppliChem GmbH	 Darmstadt, Germany

2.1.5 Immunohistochemistry

Product name	Product nº	Company	Provenance
Acetone	24201	Sigma-Aldrich, Inc.	St.Louis, MO, USA

Product name	Product nº	Company	Provenance
biotinylated anti rabbit IgG		Vector Laboratories	CA, USA
CD41 rabbit anti-mouse Ab	ab63983	Abcam	Cambridge, UK
Confocal laser scanning microscope LSM 510 Meta ^{MK4}	-	Carl Zeiss MicroImaging GmbH	Jena, Germany
DAB substrate kit		Vector Laboratories	CA, USA
Histogreen	E109	Linaris	Wertheim, Germany
MBT pap pen	297840010	Micro-Bio-Tec-Brand	Giessen, Germany
Nuclear fast red	H3403	Linaris	Wertheim, Germany
PBS tablets	18912-014	Invitrogen Corp.- Gibco	Carlsbad, CA, USA
Rat anti-mouse neutrophil antibody	MCA771G	AbD Serotec	Düsseldorf, Germany
SuperFrost plus object plate	03-0060	R. Langenbrinck Labor- und Medizintechnik	Emmendingen, Germany
Vectastain ABC Kit		Vector Laboratories	CA, USA
Xylene	28975.325	VWR International S.A.S	Briare, France

2.1.6 Animal experiments

Product name	Product nº	Company	Provenance
0,9% sodium chloride		Fresenius Mediacal Care AG & Co	Hof a.d. Saale, Germany
ANP		Sigma-Aldrich	Munich, Germany
Chrono-Lume®		Chrono-Log Corp.	Havertown, USA
Evan's blue			
PGE1		Sigma-Aldrich	Munich, Germany

Product name	Product nº	Company	Provenance
Prolene 8.0		Ethicon	Norderstedt, Germany
Purified anti-mouse Ly-6G functional grade		eBioscience	Frankfurt, Germany
Rabbit anti-mouse thrombozyte antiserum		WAK-Chemie Medical GmbH	Steinbach, Germany
Servo 900C		Siemens	Germany
Tetracycline (100 mg/l)		Uniapotheke	
VASP ON-TARGETplus SMARTpool Mouse siRNA	J-046659-17 J-046659-18 J-046659-19 J-046659-20	Thermo Scientific	Dreieich, Germany
WT mice (C57BL/6J)			
VASP knockout mice			

2.1.7 Cell culture

Product name	Product nº	Company	Provenance
Accutase	L11-007	PAA Laboratories GmbH	Pasching, Austria
Antibiotic-Antimycotic Solution	A5955	Sigma-Aldrich Inc.	St.Louis, MO, USA
Cell Culture Plate 6 well 12 well 24 well	 3506 3512 3527	Corning Inc. Life Sciences	Lowell, MA, USA
Cell Lifter Cell Scraper	3008 3010	Corning Inc. Life Sciences	Lowell, MA, USA
Cytoperm 2	51011660	Heraeus Instruments GmbH	Hanau, Germany
Diaphragm Vacuum Pump	18807 417	Vacuubrand GmbH + Co. KG	Wertheim, Germany
D-PBS 1x (+CaCl2) (+MgCl2)	14040	Invitrogen Corp.-Gibco	Carlsbad, CA, USA

Product name	Product nº	Company	Provenance
D-PBS 1x (-CaCl2) (-MgCl2)	14190	Invitrogen Corp.- Gibco	Carlsbad, CA, USA
Endothelial Cell Growth Medium MV	C-22020	Promocell	Heidelberg, Germany
F-12 Nutrient Mixture (Ham)1x	21765	Invitrogen Corp.- Gibco	Carlsbad, CA, USA
Foetal Bovine Serum GOLD	A15-151	PAA Laboratories GmbH	Pasching, Austria
G-418 disulfate salt solution	G8168	Sigma-Aldrich Inc.	St.Louis, MO, USA
G418-Bc Sulfate Powder Subst.	A291-25	Biochrom	Berlin, Germany
hEGF	354052	Becton Dickinson	Franklin Lakes, NJ, USA
HMEC-1 human microvascular endothelial cells	-	Gift of Sean Colgan	Denver, CO, USA
Hydrocortisone	354203	Becton Dickinson	Franklin Lakes, NJ, USA
LaminAir HB 2472 S GS	50033854	Heraeus Instruments GmbH	Hanau, Germany
L-Glutamine 200 mM 100x	25030-024	Invitrogen Corp.- Gibco	Carlsbad, CA, USA
MCDB 131 1x	10372	Invitrogen Corp.- Gibco	Carlsbad, CA, USA
Microscope DMIL	090-131.001	Leica Mikroskopie & Systeme GmbH	Wetzlar, Germany
Mycoplasma removal agent (MRA)	BUF035	Serotec Ltd.	Oxford, UK
Supplement Mix / Endothelial Cell Growth Medium MV	C-39225	Promocell	Heidelberg, Germany
Tissue Culture Dishes		Greiner Bio-One	Frickenhausen,

Product name	Product nº	Company	Provenance
35x10 mm 60x15 mm 94x16 mm	627 160 628 160 633 171	GmbH	Germany
Tissue Culture Flask	90076	Techno Plastic Products AG	Trasadingen, Switzerland
Trypan Blue solution	T8154	Sigma-Aldrich Inc.	St.Louis, MO, USA
Venor GeM-qEP Mycoplasma Detection	11-4100	Minerva Biolabs GmbH	Berlin, Germany

2.2 Methods

2.2.1 Western blots for VASP and VASP phosphorylation.

Neutrophils in the presence of platelets were stimulated with either 10µM ANP or 10µM PGE1 and lysed. After spinning at 14,000xg for 10 min to remove cell debris, the pellet was resuspended in RIPA buffer and protein concentration was measured. Primary antibodies were for VASP (Cell Signaling, distributed by New England Biolabs, Frankfurt am Main, Germany), pVASP^{157} (Cell Signaling, distributed by New England Biolabs, Frankfurt am Main, Germany) and pVASP^{239} (Cell Signaling, distributed by New England Biolabs, Frankfurt am Main, Germany). Loading conditions were controlled by staining human ß-actin using a murine monoclonal antibody (Cell Signaling, distributed by New England Biolabs, Frankfurt am Main, Germany). Murine westernblot analysis was performed as described above.

2.2.2 Fluorescence activated cell sorting (FACS) -Flow cytometry

Briefly, a single cell suspension of 1×10^5 neutrophils or platelets in 100µl of PBS was incubated with saturating concentrations of indicated primary antibodies for 20 min. After three washes, the cells were centrifuged at 200g for 5 min, and resuspended in Cellfix. Fluorescence was evaluated on a FACS Calibur following stimulation with PMA, and data were analyzed by using Cell Quest software (all BD Biosciences, Heidelberg, Germany). Antibodies used

were CD41a, GPIIb/IIIa epitope PAC-1 (both BD Biosciences, Heidelberg, Germany) CD18 and CD11b (both NatuTec an eBioscience Company, Frankfurt, Germany). In a subset of experiments neutrophils and platelets were pre-incubated with PGE1 or ANP to study the impact of VASP phosphorylation.

2.2.3 Isolation of human neutrophils / platelets

Peripheral blood was taken from healthy donors into a Sarstedt Monevette containing Sodium citrate (Sarstedt, Nümbrecht, Germany).

Isolation of neutrophils. Briefly, platelets, plasma, and mononuclear cells were removed by aspiration following centrifugation through a double layer of Histopaque-T1077 and Histopaque-T1119 (Sigma-Aldrich) at 500 g for 30 minutes at 22°C. PMNs were found at the interface between T1077 and T1119. Residual erythrocytes were removed by lysis in cold NH4Cl buffer. Remaining cells were greater than 97% PMNs as assessed by microscopic evaluation. PMNs were studied within 2 hours of their isolation.[73-74]

Isolation of platelets. Platelet-rich plasma was obtained from whole blood anticoagulated with sodium citrate, diluted with ACD puffer following centrifugation at 150 g for 15 minutes at 22°C. Numbers of platelets were assessed by microscopic evaluation. One milliliter of platelet-rich plasma was resuspended in 5 ml HBSS minus and centrifuged at 1,400 g for 10 minutes at 4°C. Platelets were studied within 2 hours of their isolation.[67]

2.2.4 Transendothelial migration assay (TEM)

Migration assays were performed in the absence or presence of platelets. Briefly, 5×10^5 neutrophils were added together with 2.5×10^7 platelets to the upper chamber of transwell inserts (Costar, Amsterdam, Netherlands) in which HMEC-1 cell monolayers were seeded on the apical aspect. A chemotactic gradient was established by adding 1 µM Phorbol 12-myristate 13-acetate (PMA) to the lower chambers. Transmigration studies were performed in the presence of CD11b antibody (Pharmingen, Heidelberg, Germany) or GPIIb/IIIa antagonist ReoPro® (Gießen, Germany). In a subset of experiments neutrophils

and platelets were pre-incubated with PGE1 or ANP to study the impact of VASP phosphorylation on translocation.

2.2.5 Immunohistochemistry of neutrophils and platelets in murine tissue

Immunohistochemical staining was performed with Vectastain ABC Kit (Linaris, Wertheim, Germany). After inhibiting the non-specific binding sites with Avidin Blocking solution (Vector Laboratories, CA, USA) the sections were incubated with primary antibody (rabbit anti-mouse CD41, Abcam, Cambridge, UK) over night at 4°C. Tissue sections were then incubated with biotinylated anti rabbit IgG for 1 hour followed by Vectastain ABC Reagent for 30 minutes, and then developed using DAB substrate. For neutrophil staining, the procedure was repeated using rat anti-mouse neutrophil antibody (AbD Serotec, Düsseldorf, Germany) and histogreen as substrate (Linaris, Wertheim, Germany). Counterstaining was performed using nuclear fast red (Linaris, Wertheim, Germany).

2.2.6 Animal experiments

2.2.6.1 Mice.

All animal protocols were in accordance with the German guidelines for use of living animals and were approved by the Institutional Animal Care and Use Committee of the Tübingen University Hospital and the Regierungspräsidium Tübingen. *VASP*$^{-/-}$ mice were generated, validated and characterized as described previously.[74-75] The WT controls (C57BL/6J mice) were bred as littermates of *VASP*$^{-/-}$ mice.

2.2.6.2 Murine model of myocardial ischemia.

VASP$^{-/-}$ mice and littermate controls were matched in age, gender and weight. After anesthesia was induced animals were placed on a temperature-controlled and heated table to maintain body temperature at 37°C. Animals were orally intubated and ventilated (Servo 900C, Siemens, Germany). Following left parasternal thoracotomy, the left coronary artery (LCA) was visually identified

and an 8.0 nylon suture (Prolene, Ethicon, Norderstedt, Germany) was placed around the vessel, ischemia induced using a model described previously.[76] Infarct sizes were determined by calculating the percentage of myocardial infarction compared to the area at risk (AAR) using double staining technique with Evan's blue and triphenyltetrazolium chloride (TTC).[77] AAR and the infarct size were determined via planimetry using NIH software Image 1.0 and the degree of myocardial damage was calculated as percentage of infarcted myocardium from the AAR.

2.2.6.3 Generation of bone marrow (BM) chimeras.

In short, male donor mice (8-10 weeks old, 20-25g) were euthanized, marrow harvested by flushing the marrow cavity and bone marrow cells were then centrifuged at 400xg for 5 minutes, resuspended and counted. Recipient mice (8–10 weeks of age, 20–25 g) were irradiated with a total dose of 12 Gy from a 137Cs source. Immediately after irradiation, 10^7 BM cells/recipient were injected in 0.2 ml 0.9% sodium chloride into the jugular vein. The resulting chimeric mice were housed in microisolators for at least 8 weeks before experimentation and fed with water containing tetracycline (100 mg/l) in the first two weeks following BM transplantation. Bone marrow cells were transplanted to generate (1) [WT → WT] (2) [*VASP*$^{-/-}$ → *VASP*$^{-/-}$] mice as controls and (3) [WT → *VASP*$^{-/-}$] (4) [*VASP*$^{-/-}$ → WT] chimeric mice (47).

2.2.6.4 Pharmacological compounds used.

Prostaglandin E_1 (PGE_1) (0.14 µg/kg/h, Sigma-Aldrich, Munich, Germany), Atrial natriuretic peptide (ANP) (0.04 µg/kg/h, Sigma-Aldrich, Munich, Germany) or vehicle (0.9% NaCl) was administered by intra-arterial infusion beginning 5 min prior to reperfusion.

2.2.6.5 *In-vivo* Small Interfering RNA Repression.

To achieve *in-vivo* repression of VASP we used 2.2µg/g body weight VASP ON-TARGETplus SMARTpool Mouse siRNA dissolved in 5% Glucose-solution. As control non-targeting siRNA (Thermo Scientific, Dreieich Germany) with at least four mismatches to any human, murine or rat gene. The siRNA target

sequences of the VASP pool were, J-046659-17 with target sequence UGC AUU CUG AGC AAA, J-046659-18 with target sequence AGG AAA UCA UCG AAG UCU U, J-046659-19 with target sequence GGG CUA CUG UGA UGC UUU A, J-046659-20 with target sequence GAG CUG AGG AAG CGG GGU U.

2.2.6.6 *In-vivo* depletion of murine neutrophils and platelets.

We achieved neutrophil depletion using neutrophil-specific antibody treatment (purified anti-mouse Ly-6G functional grade; 200µg/mouse, intravenously (i.v.); eBioscience, Frankfurt) 24 hours before experiments. We achieved platelet depletion using an adsorbed rabbit anti-mouse thrombocyte antiserum (50µl/mouse i.v.; WAK-Chemie Medical GmbH) 2 hours before experiments.

2.2.6.7 Platelet cross over injection.

Platelets were separated as described previously.[67] Platelets were counted and 1.2 x 10^6 platelets per mouse were injected into the carotid artery at the start of the surgical procedure (in 200µl volume). Prior to injection, platelets were tested as to whether activation was possible through thrombin and ATP release determined through luciferase (Chrono-Lume®, Chrono-Log Corp., Havertown, USA).

2.2.7 Troponin I Measurement.

Blood was collected by central venous puncture for troponin I (cTnI) measurements using a quantitative rapid cTnI assay (Life Diagnostics, Inc, West Chester, Pa).

2.2.8 Shear Stress and Live Cell Imaging.

Live cell imaging was performed using CellTracker™ Green CMFDA (5-chloromethylfluorescein diacetate) for neutrophils or CellTracker™ Red CMTPX, (Invitrogen, Karlsruhe, Germany) for platelets according to the protocol the manufacturer provided. Cells were incubated for 30 minutes at 37°C, centrifuged at 250g for 10 minutes and incubated with dye for additional 30 minutes. For imaging cells were filled in Ibidi µ-Slide $VI^{0.1}$ (Ibidi, Martinsried, Germany) and confocal microscopy was performed with Zeiss AxioObserver Z1

(Zeiss, Jena, Germany) microscope was equipped with Apotome employing AxioVision 4.6 software (Zeiss, Jena, Germany).

2.2.9 Data analysis.

Data were compared by ANOVA, or by Student's *t* test where appropriate. Values are expressed as the mean ± SEM. A $p<0.05$ was considered to be statistically significant.

3 Results

3.1 VASP phosphorylation affects neutrophil facilitated transendothelial platelet movement.

During myocardial IR injury neutrophils as well as platelets are known to affect the extent of the associated reperfusion injury. The importance of PNC formation has been reported by previous studies.[66-67] To test the impact of PNC formation and to define controlling mechanisms involved into PNC formation, we initially performed transendothelial movement studies.

In an initial experiment we stimulated isolated neutrophils or platelets using a chemotactic gradient across an endothelial monolayer, and found that neutrophils readily migrate across endothelial monolyers in response to phorbol 12-mystrate 13acetate (PMA) stimulation. Platelets did not demonstrate increased transendothelial movement in response to PMA stimulation. When exposing neutrophils and platelets together to PMA stimulation, a robust increase of cells and of ATP content could be found in the basolateral compartment. A firm link between neutrophils and platelets is largely dependent on the interaction of CD11b/CD18 on neutrophils and the GPIIb/IIIa receptor on platelets.[14] We therefore pre-exposed neutrophils and platelets to either CD11b antibody or GPIIb/IIIa antagonist ReoPro® prior to transendothelial movement studies and found a significant decrease of neutrophils and ATP content in the basolateral compartment (Figure 6A and B, Figure 7).

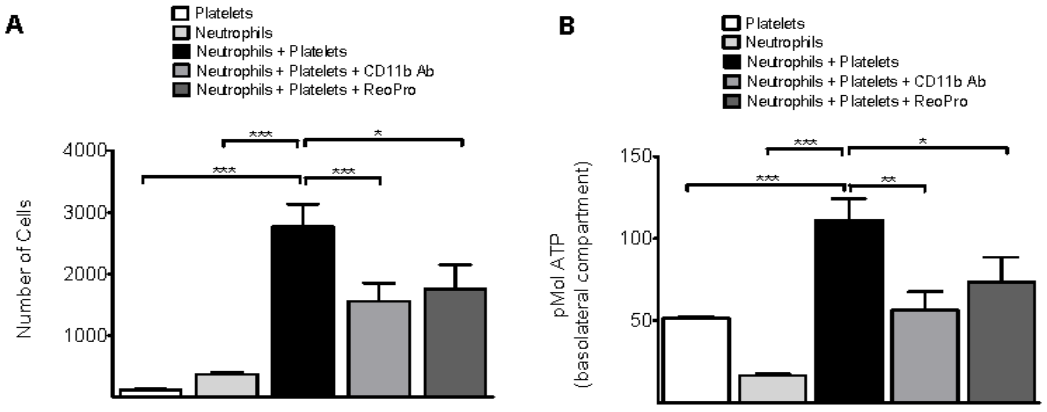

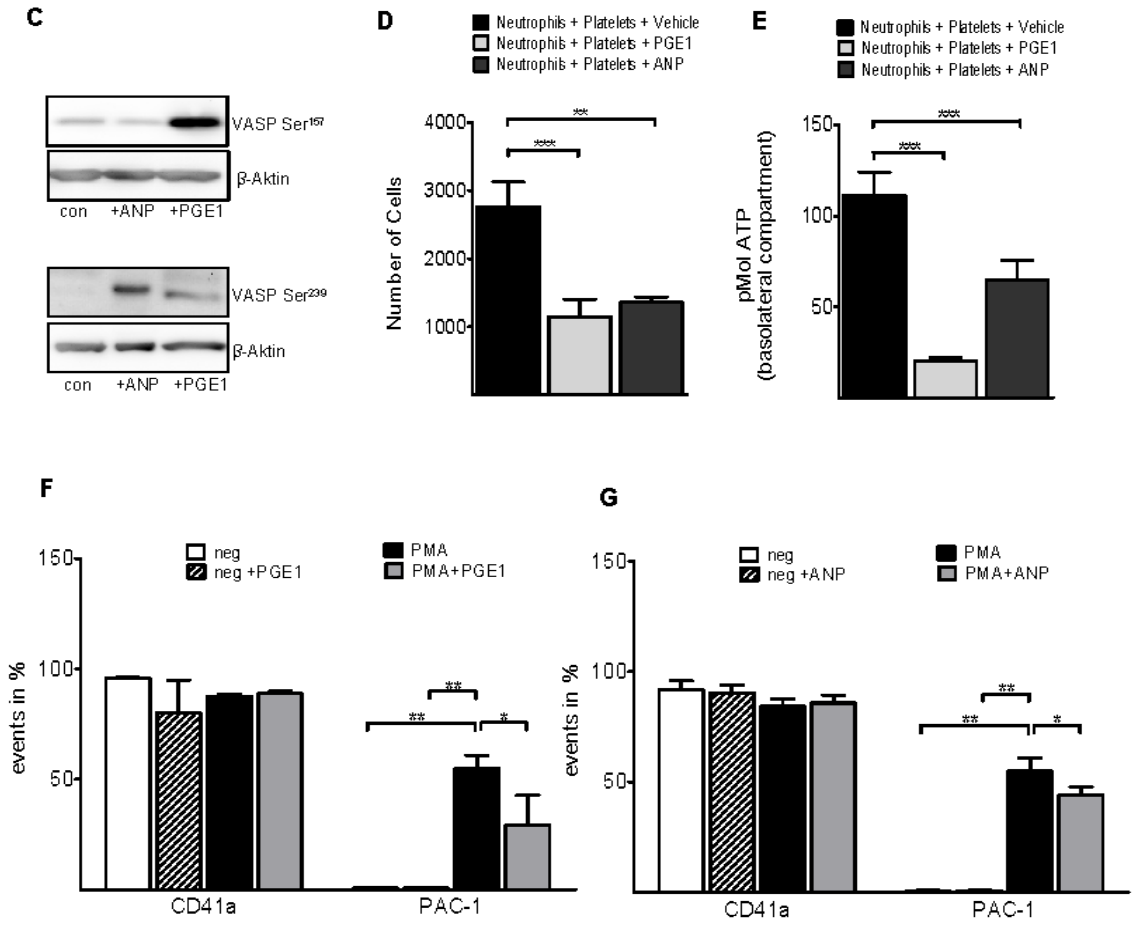

Figure 6 – VASP phosphorylation reduces neutrophil facilitated transendothelial platelet-movement.

Neutrophils ($5x10^5$) and platelets ($2,5×10^7$) were incubated in the presence or absence of either CD11b antibody or GPIIb/IIIa antagonist (ReoPro®) in the apical compartment. PMA (1 µM) was present in the basolateral compartment to induce a chemotactic gradient. Translocation across endothelial HMEC-1 was determined by the presence of cell count or ATP concentration in the basolateral compartment after 60 minutes. **A)** Cell number in the basolateral compartment was determined via myeloperoxidase assay (MPO) **B)** ATP content in the basolatateral compartment **C)** VASP phosphorylation in neutrophil-platelet suspension following stimulation with prostaglandin E1 (PGE1) to induce VASP Ser-157 and atrial natriuretic peptide (ANP) to induce VASP Ser-239 phosphorylation **D)** Number of cells in the basolateral compartment after pre-incubation with either PGE1 or ANP and PMA in the basolateral compartment as determined by MPO assay **E)** ATP content in the basolateral compartment after pre-incubation with either PGE1 or ANP and PMA in the basolateral compartment **F)** Expression of CD41a or PAC-1 on the surface of platelets pre-incubated with PGE1 prior to stimulation with PMA determined by flowcytometry **G)** Expression of CD41a or PAC-1 on the surface of platelets pre-incubated with ANP prior to stimulation with PMA determined by flowcytometry (data are

shown as mean ± SEM, n= 12-16 per group for transendothelial studies, n=3 for flowcytometry, **P* < 0.05; ***P* < 0.01,. ****P* < 0.001 as indicated)

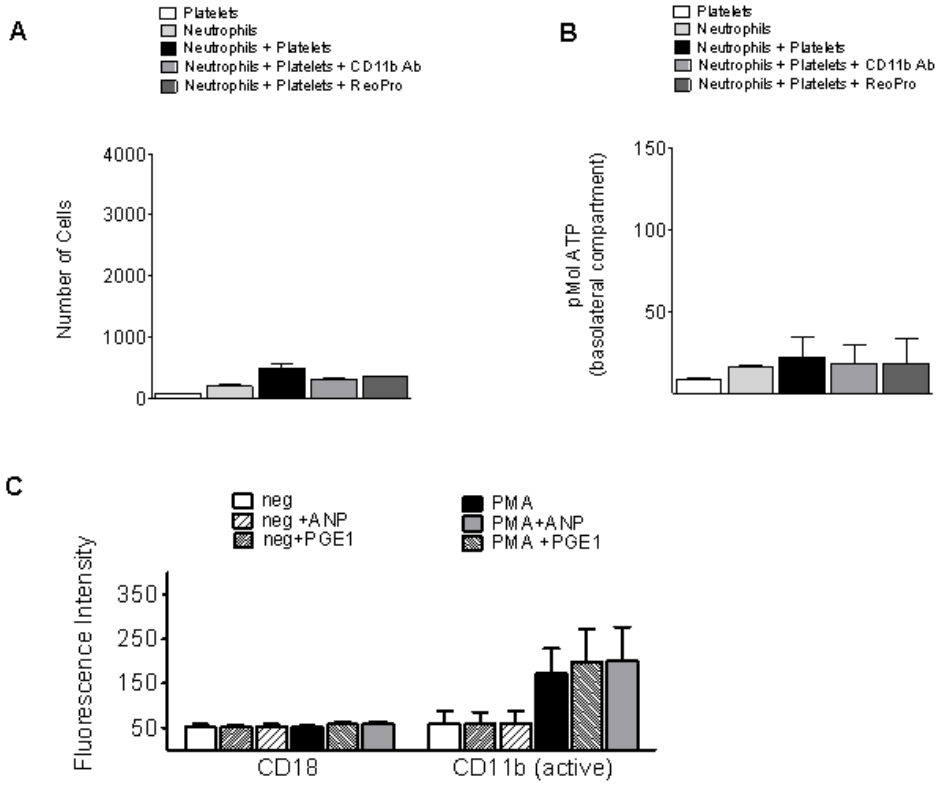

Figure 7 – Passive movement of platelets or neutrophils across endothelial monolayers, and expression of CD18 and CD11b on the surface of neutrophils in response to PMA. Neutrophils ($5x10^5$) and platelets ($2,5×10^7$) were incubated in the presence or absence of either CD11b antibody or GPIIb/IIIa antagonist (ReoPro®) in the apical compartment. Translocation across endothelial HMEC-1 was determined by the presence of cell count or ATP concentration in the basolateral compartment after 60 minutes. **A)** Cell number in the basolateral compartment was determined via myeloperoxidase assay (MPO). **B)** ATP content in the basolatateral compartment. **C)** Fluorescence intensity of CD18 and CD11b on the surface of neutrophils pre-incubated with PGE1 or ANP prior to stimulation with PMA determined by flowcytometry (Results are obtained from 6 monolayers in each condition; n=3 for flowcytometry, data are mean ± SEM)

Previous work has implicated that actin dynamics influence the exposure of CD11b/CD18 or GPIIb/IIIa.[71,78] A crucial regulator of actin dynamics is VASP, and phosphorylation of VASP rapidly mediates platelet shape changes.[79] VASP contains 3 possible phosphorylation sites (Ser-157, Ser-239 and Thr-278), and

two of these are described to be important determinants of platelet function (Ser-157 and Ser-239). We therefore proceeded to selectively phosphorylate the VASP Ser-157 site (through PGE1) and the VASP Ser-239 site (through ANP) to pursue its role on neutrophil facilitated transendothelial platelet movement (Figure 6C). Following pre-incubation of the neutrophil-platelet suspension with PGE1 or ANP we found a significant reduction of cell number and ATP concentration within the basolateral compartment (Figure 6D and E). To gain further insight into this process, we determined whether the activated form of the GPIIb/IIIa receptor, GPIIb/IIIa and activated CD11b would be affected by PGE1 or ANP pre-treatment. Following pre-incubation with PGE1 or ANP we found a significant reduction of PAC-1 on the surface of platelets following stimulation with PMA but did not find a change in the expression of CD11b (Figure 6F and G, Figure 7).

Reperfusion of the myocardium produces shear stress at the affected tissue site. This shear stress induces an activation of platelets. Therefore, we proceeded to co-incubate platelets with neutrophils under shear stress generated through centrifugation at 250g. We added either vehicle, PGE1 or ANP to this process. Following centrifugation we found platelets to outline the surface of neutrophils through attachment on their surface (Figure 8B). After incubation with PGE1 or ANP platelets did not attach to the surface of neutrophils (Figure 8C and D).

3.2 VASP deficient mice demonstrate reduced PNCs and decreased myocardial IR injury.

We then proceeded to investigate whether this finding could have *in-vivo* significance and proceeded to use a model of myocardial IR injury. We exposed previously characterized *VASP*$^{-/-}$ and littermate controls to 60 minutes of myocardial ischemia followed by 3 hours of reperfusion. We found *VASP*$^{-/-}$ mice to demonstrate a significant reduction of myocardial infarct size compared to controls; this was corroborated through serum troponin I (cTnI) levels (Figure

9A to C). We then examined tissue sections of the affected myocardium for the presence of PNCs within infarcted tissue and found a reduced presence of PNCs within tissue of *VASP*$^{-/-}$ animals compared to littermate controls (Figure 9D).

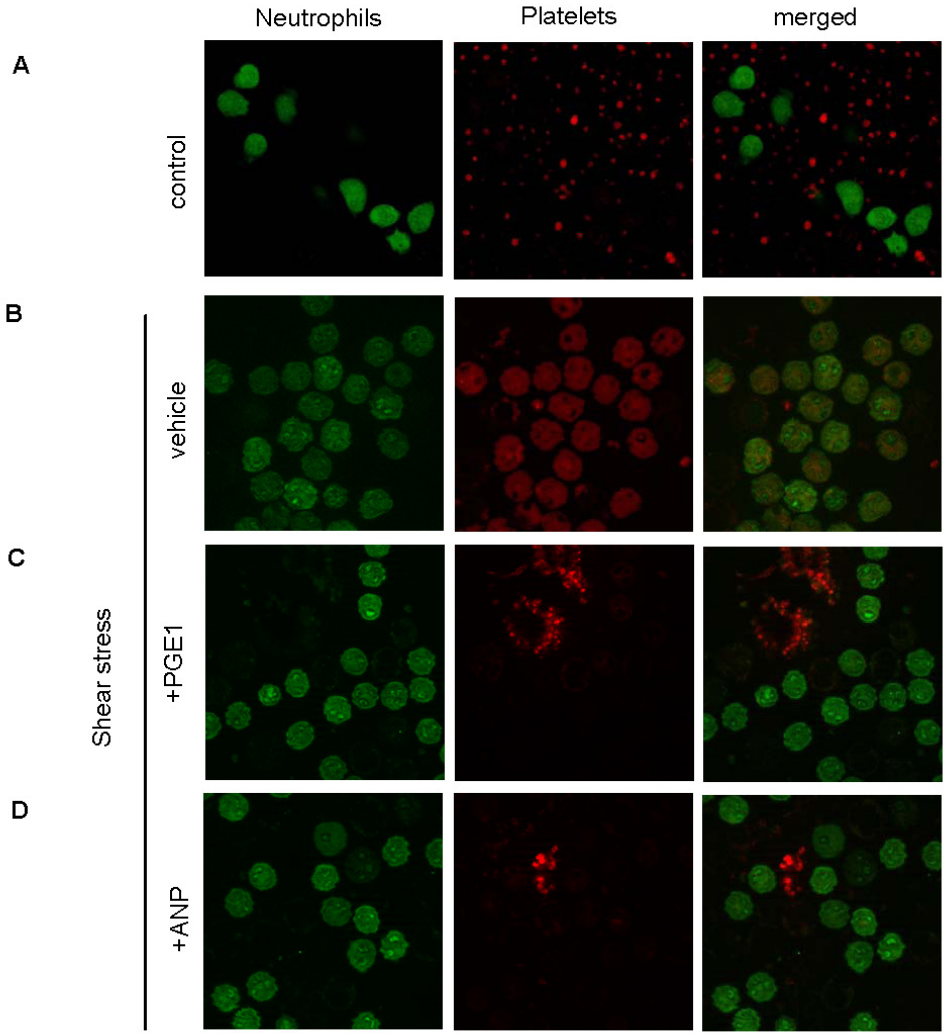

Figure 8 – Shear stress induces PNC formation.

Platelets and neutrophils were labeled with CellTracker^{TM} Red CMTPX and CellTracker^{TM} Green, CMFDA, respectively. Platelets (2.5×10^7) were incubated with neutrophils (5×10^5; 1 µM PMA) in the presence or absence of either PGE1 or ANP, activated via centrifugation (250 x g) and live cell imaging of neutrophils (green) and platelets (red) performed following **A)** No centrifugation, **B)** After centrifugation and vehicle exposure **C)** After centrifugation in the presence of PGE1 **D)** After centrifugation in the presence of ANP (One representative of 3 individual experiments is demonstrated)

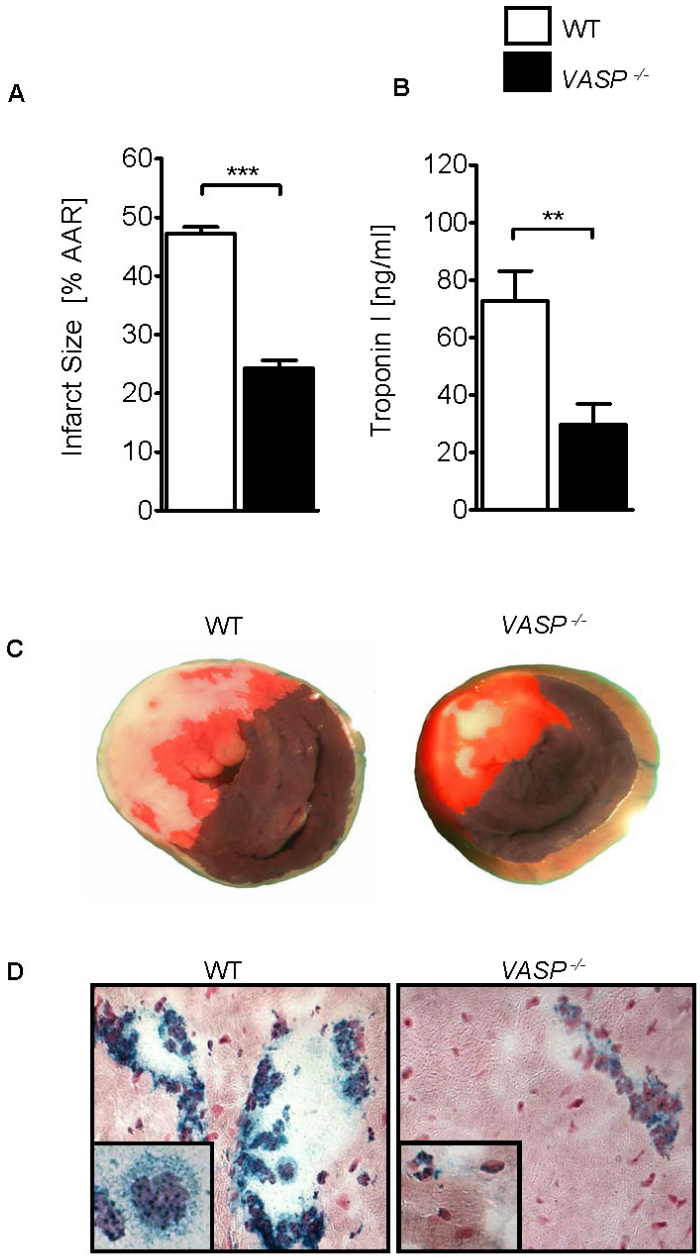

Figure 9 – *VASP*$^{-/-}$ animals demonstrate reduced presence of PNCs and reduced myocardial IR injury.

A) Infarct size in *VASP*$^{-/-}$ mice in comparison to WT mice after 60 minutes of myocardial ischemia followed by 2 hours reperfusion. Calculated is the percentage of necrotic tissue to the area at risk (AAR). **B)** Depicted are correlating serum troponin I measurement of *VASP*$^{-/-}$ and WT animals. **C)** Representative images of myocardial infarcts (blue/dark= retrograde Evan's blue staining; red and white= area at risk; white= infarcted tissue) **D)** Histological images of platelet-neutrophil complexes (neutrophil = blue; platelet = black) in tissue sections of myocardial infarct of *VASP*$^{-/-}$ and WT animals (data are shown as mean ± SEM, n=6, $^{**}P < 0.01$; $^{***}P < 0.001$ as indicated, tissue sections magnification x400 and x1000, n=3, one representative of 3 individual experiments is demonstrated).

To gain further insight into the specific role of VASP we employed gene targeted repression using siRNA and injected animals 24 hours prior to the start of the experiment with siVASP or control siRNA (siSCR). This resulted in significant VASP repression *in-vivo* (Figure 10). We then proceeded to subject these animals to the myocardial IR model and found reduced myocardial tissue damage in the siVASP treated animals compared to siSCR controls (Figure 11A to C). This reduced myocardial damage was associated with a reduced presence of PNCs within then affected myocardial tissue (Figure 11D).

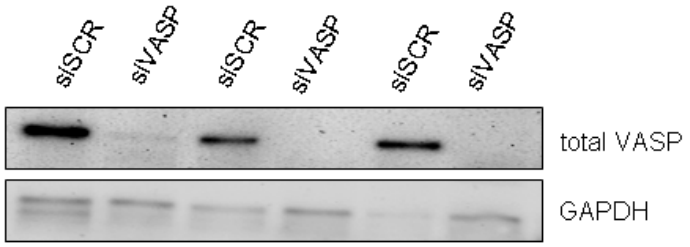

Figure 10 – VASP expression following siRNA injection.
Westernblot analysis of 3 individual WT animals 24h post siVASP or siSCR injection.

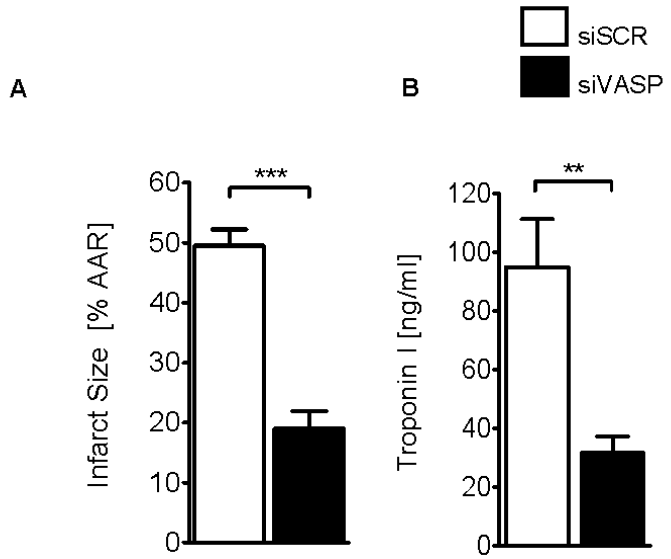

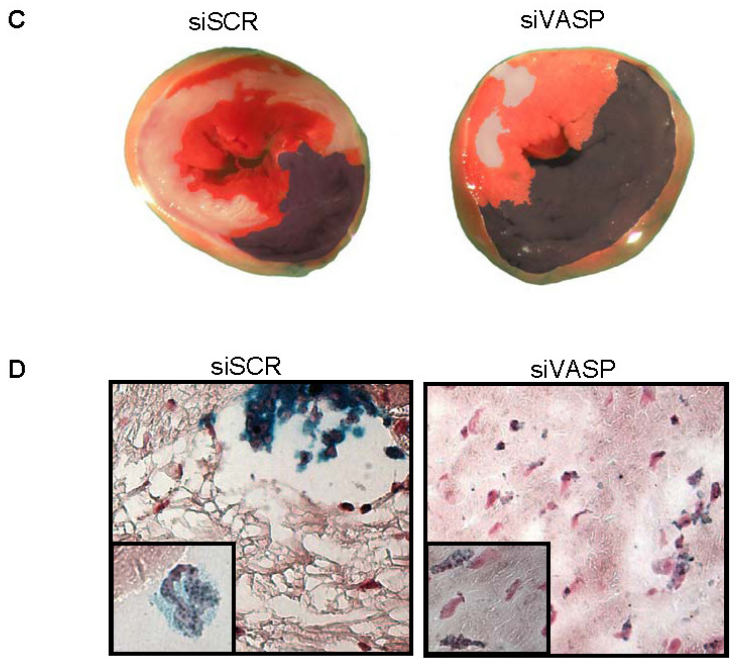

Figure 11 – *In-vivo* VASP repression by siRNA dampens myocardial IR injury.

A) Myocardial IR Injury after *in-vivo* targeted repression of VASP with siRNA (siVASP) or non-targeting siRNA (siSCR) and **B)** Depicted are correlating serum troponin I values. **C)** Representative images of myocardial infarcts (blue/dark= retrograde Evan's blue staining; red and white= area at risk; white= infarcted tissue). **D)** Histological images of platelet-neutrophil complexes (neutrophil = blue; platelet = black) in tissue sections of myocardial infarct of siSCR or siVASP treated WT animals after IR (data are shown as mean ± SEM, n=6, $^{**}P < 0.01$; $^{***}P < 0.001$ as indicated, tissue sections magnification x400 and x1000, n=3, one representative of 3 individual experiments is demonstrated).

3.3 PNC formation is dependent on hematopoietic VASP expression.

To further clarify the role of VASP on myocardial IR injury and the formation of PNCs we generated chimeric animals using bone marrow transplantation (Figure 12). 6 weeks following bone marrow transplantation, we performed the above described myocardial IR model. In chimeric animals myocardial IR injury was dependent on hematopoietic VASP expression, demonstrating reduced myocardial damage in the $VASP^{-/-}$→WT transplanted animals. The control transplanted animals (WT→WT and $VASP^{-/-}$→$VASP^{-/-}$) reflected the results of the WT or $VASP^{-/-}$ animals (Figure 13A to C). These findings were confirmed by serum troponin I levels. When examining myocardial tissue sections for the

presence of PNC's we found that *VASP*$^{-/-}$→WT transplanted animals showed a reduced presence of PNCs compared to the WT→*VASP*$^{-/-}$ transplanted animals which was associated with an increase in myocardial tissue destruction (Figure 13D).

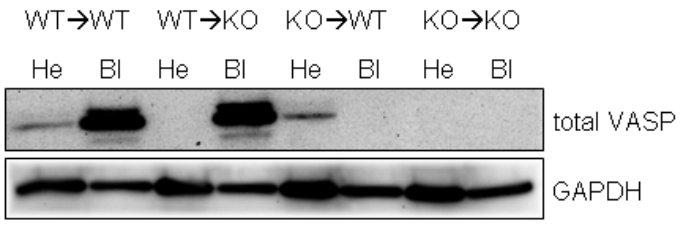

Figure 12 – VASP expression in chimeric animals.

Westernblot analysis of chimeric animals following bone marrow transplantation demonstrating VASP expression in the myocardium and blood of WT→WT transplanted animals, hematopoietic WT in *VASP*$^{-/-}$ animals (WT→*VASP*$^{-/-}$), hematopoietic *VASP*$^{-/-}$ in WT animals (*VASP*$^{-/-}$→WT), and *VASP*$^{-/-}$ →*VASP*$^{-/-}$ transplanted control animals (pooled samples of n=4/ group).

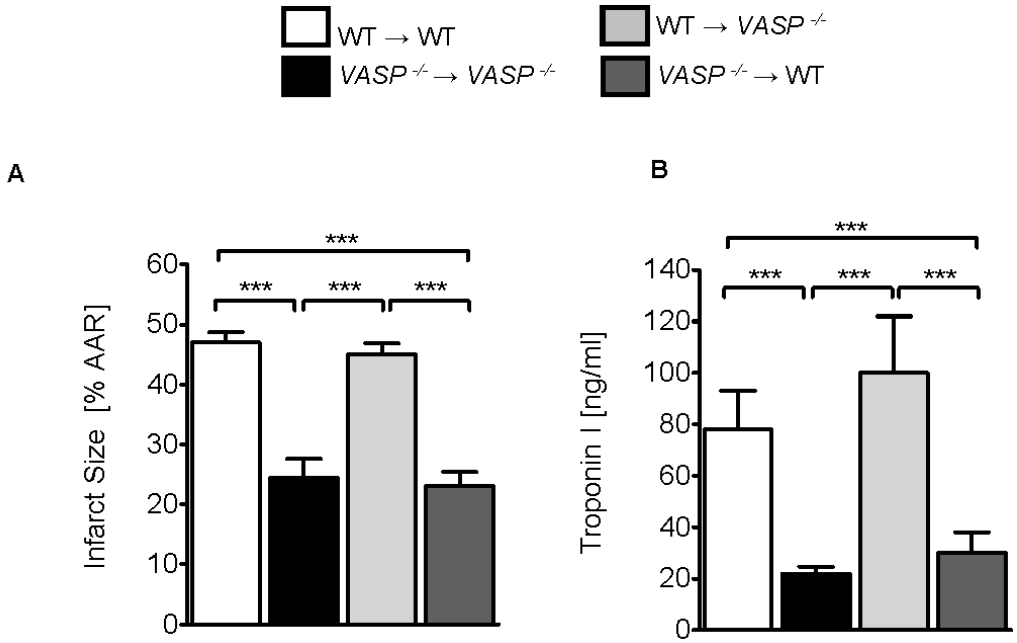

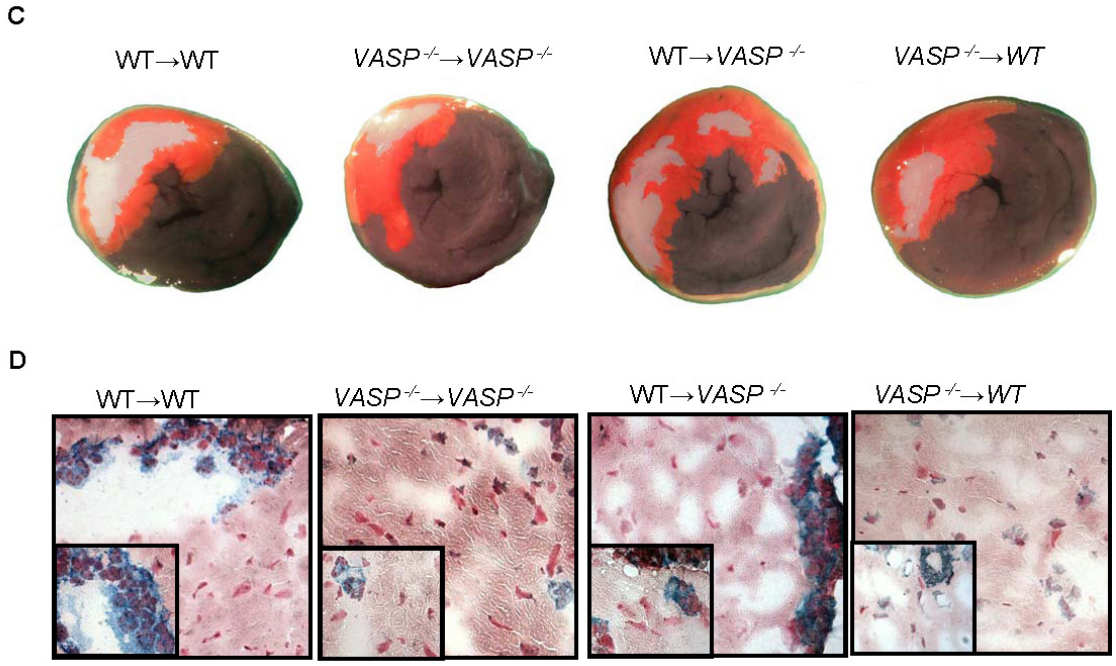

Figure 13 – PNCs and myocardial IR injury in chimeric animals.

A) Infarct size in chimeric animals (*VASP*$^{-/-}$→WT and WT→*VASP*$^{-/-}$) and control transplanted animals after 60 min of myocardial ischemia followed by 2 hours reperfusion. The percentage of necrotic tissue to the area at risk (AAR) is shown and **B)** Correlating serum troponin I values are depicted. **C**) Representative images of myocardial infarcts (blue/dark= retrograde Evan's blue staining; red and white= area at risk; white= infarcted tissue). **D**) Histological images of platelet-neutrophil complexes (neutrophil = blue; platelets = black) in tissue sections of myocardial infarct of chimeric animals (*VASP*$^{-/-}$→WT and WT→*VASP*$^{-/-}$) (data are shown as mean ± SEM, n=6, **P* < 0.05; ***P* < 0.01,. ****P* < 0.001 as indicated, tissue sections magnification x400 and x1000, n=3, one representative of 3 individual experiments is demonstrated).

3.4 Depletion of platelets or neutrophils dampens myocardial IR injury in WT and VASP$^{-/-}$ mice.

To gain further insight whether the observed protective effect of VASP depletion is indeed mediated through the formation of PNCs, we selectively depleted platelets from animals and exposed them to the model of myocardial IR injury. Platelet depletion resulted in a significant reduction of myocardial IR injury in WT and in *VASP*$^{-/-}$ animals. WT animals demonstrated an infarct size of 4.5±2.4% , *VASP*$^{-/-}$ animals of 3.5±1.4% (Figure 14A and C). When examining

tissue sections following myocardial IR injury, we did not find evidence for the presence of PNCs within the tissue sections of WT or *VASP*$^{-/-}$ animals (Figure 14E). Depletion of neutrophils resulted in a similar finding, myocardial infarct size was significantly reduced in WT animals (5.4±1.4%) and in *VASP*$^{-/-}$ animals (5.3±1.3%) (Figure 14B and D). PNC were not present within myocardial tissue, corroborating the important role of PNCs for myocardial IR injury (Figure 14F).

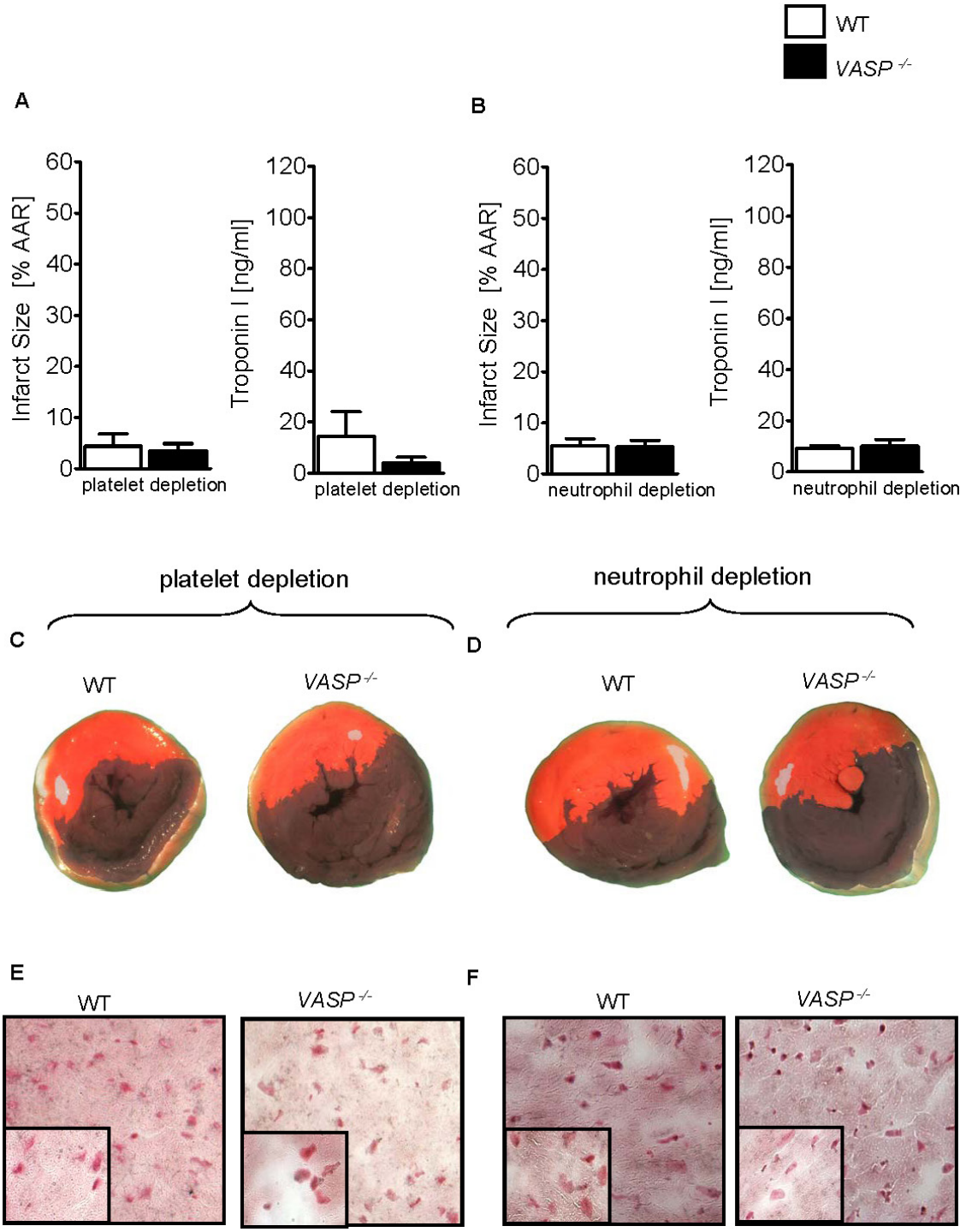

Figure 14 – Role of platelet or neutrophil depletion in WT and *VASP*$^{-/-}$ mice.
A) Myocardial IR injury in WT and *VASP*$^{-/-}$ animals following platelet depletion. Infarct sizes were measured by double staining with Evan's blue and triphenyltetrazolium chloride after 2 hours of reperfusion and correlating serum troponin I values **B)** Myocardial ischemia in WT and *VASP*$^{-/-}$ animals following neutrophil depletion and IR. Infarct sizes were measured by double staining with Evan's blue and triphenyltetrazolium chloride after 60 minutes of ischemia and 2h of reperfusion and correlating serum troponin I values **C)** Representative images of myocardial sections of infarcts following platelet depletion (blue/dark, retrograde Evan's blue staining; red and white, area at risk; white, infarcted tissue) **D)** Representative images of myocardial sections of infarcts following neutrophil depletion (blue/dark, retrograde Evan's blue staining; red and white, area at risk; white, infarcted tissue) **E)** Platelet-neutrophil complexes in WT and *VASP*$^{-/-}$ animals following platelet depletion (neutrophil = blue; platelet = black) **F)** Platelet-neutrophil complexes in WT and *VASP*$^{-/-}$ animals following neutrophil depletion after 60 minutes of ischemia and 2h of reperfusion (neutrophil = blue; platelet = black) (data are shown as mean ± SEM, n=6, tissue sections magnification x400 and x1000, n=3, one representative of 3 individual experiments is demonstrated).

3.5 PNC formation is dependent on VASP within platelets.

Inhibition of platelet function is an important therapeutic strategy during myocardial ischemia and VASP is crucially important to determine the extent of platelet activation.[80-81] Therefore, we next proceeded to clarify whether the formation of PNCs and myocardial IR injury would be influenced by VASP expression within platelets. We separated platelets from WT or *VASP*$^{-/-}$ animals to perform cross-over injection of these platelets prior to IR injury. The separation process we used did not result in an activation of the extracted platelets and separated platelets were still functionally sound (Figure 15). We then transferred *VASP*$^{-/-}$ platelets into WT animals before the start of the experiment and found that this resulted in a reduction of myocardial IR injury of approximately 40% compared to WT to WT injected animals (Figure 16A and C). In contrast, *VASP*$^{-/-}$animals injected with WT platelets demonstrated an increase in the infarct size. The reduced size of myocardial tissue damage was reflected in serum troponin I levels (Figure 16B). This was associated with a reduced presence of PNCs within WT animals receiving *VASP*$^{-/-}$ platelets and

an increased presence of PNCs in *VASP*$^{-/-}$animals injected with WT platelets within the myocardial tissue (Figure 16D).

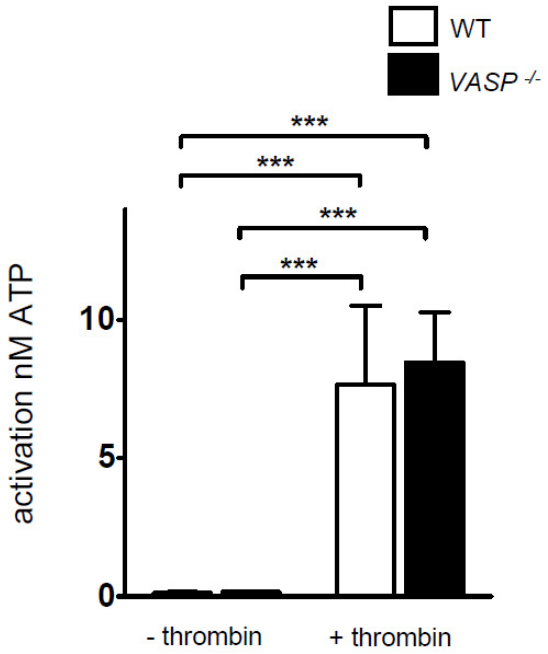

Figure 15 – Platelet separation and platelet activity.

After separation, platelets were tested for activation using luciferase dependent ATP measurement **A)** platelets prior to injection **B)** control following stimulation with thrombin to demonstrate that platelets are functionally intact and can be activated (data are mean ± SEM, n=4, ***P < 0.001 as indicated)

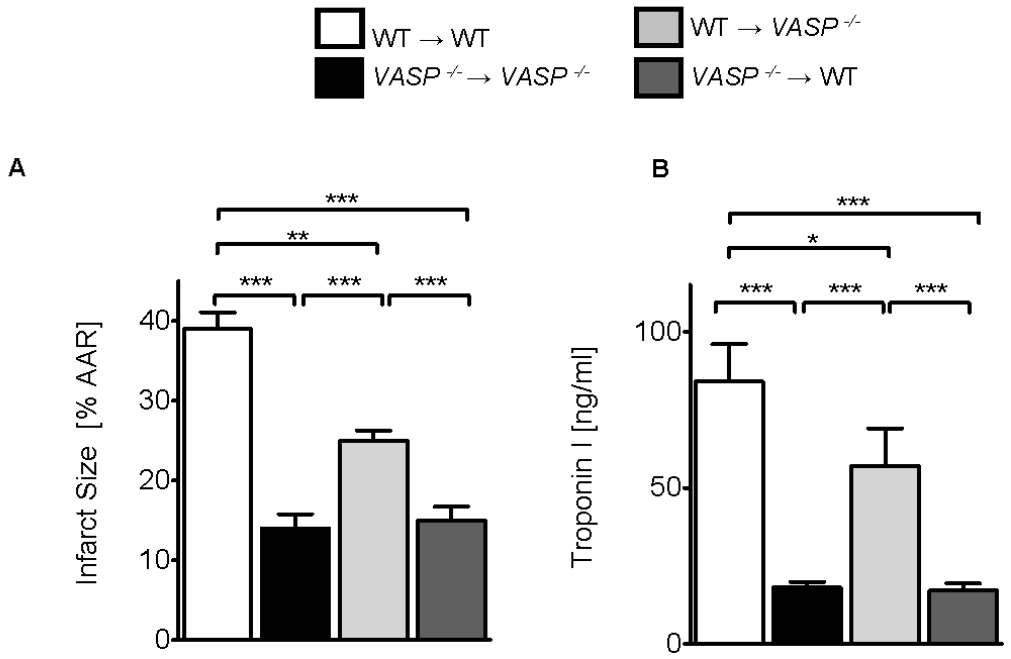

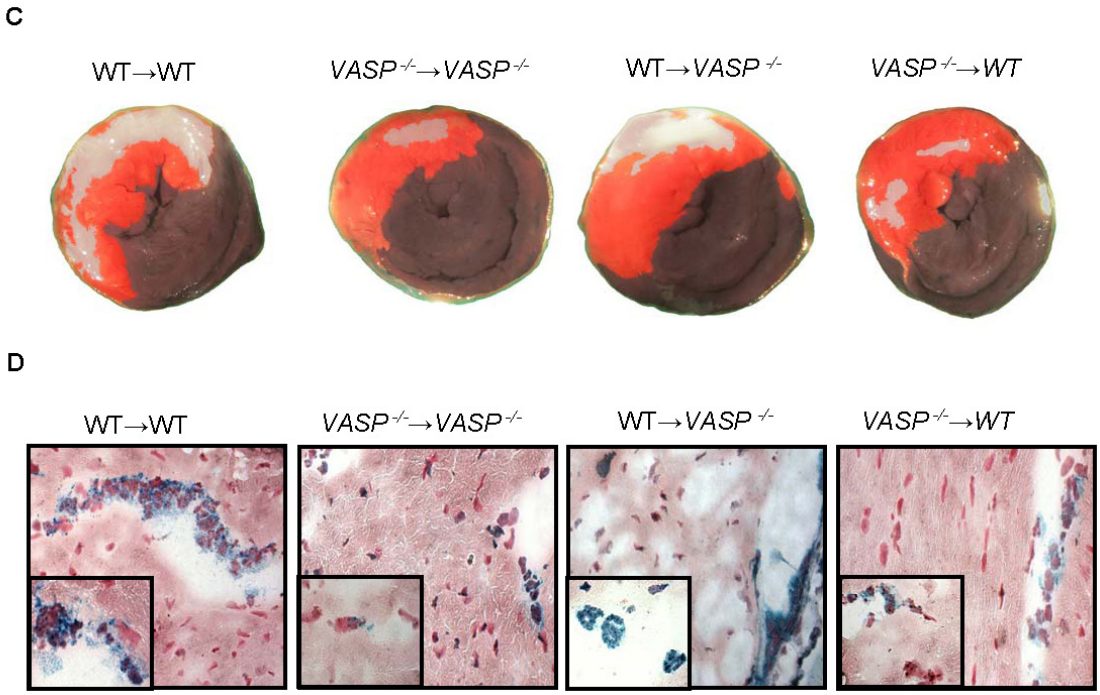

Figure 16 – Platelet cross-over injection identifies platelet-derived VASP to be crucial for PNC and myocardial IR injury.

A) Infarct size in WT and *VASP*$^{-/-}$ after platelet cross-over injection (*VASP*$^{-/-}$ into WT and WT into *VASP*$^{-/-}$ animals) and controls (WT into WT and *VASP*$^{-/-}$ into *VASP*$^{-/-}$ animals) followed by 60 minutes of myocardial ischemia and 2 hours reperfusion. The percentage of necrotic tissue to the area at risk (AAR) is shown and **B)** Correlating serum troponin I values are depicted. **C**) Representative images of myocardial infarcts (blue/dark= retrograde Evan's blue staining; red and white= area at risk; white= infarcted tissue). **D**) Histological images of platelet-neutrophil complexes (neutrophil = blue; platelet = black) in tissue sections of myocardial infarcts of all groups. (data are shown as mean ± SEM, n=6, **P* < 0.05; ***P* < 0.01; ****P* < 0.001 as indicated, tissue sections magnification x400 and x1000, n=3, one representative of 3 individual experiments is demonstrated).

3.6 VASP phosphorylation reduces myocardial IR injury.

We were able to demonstrate the *in-vitro* relevance of VASP phosphorylation for transendothelial movement of neutrophils and platelets. VASP phosphorylation is known to correlate *in-vivo* with the activation status of platelets.[82] We therefore pursued the role of the VASP phosphorylation sites *in-vivo* through employing PGE1 or ANP for the extent of myocardial IR injury and the presence of PNCs. In an initial experiment we addressed possible

hemodynamic changes following the injection but did not find a significant change of hemodynamic parameters following the injection of both proteins during the reperfusion phase (Figure 17). Infusion of PGE1 resulted in the expected murine VASP Ser-153 phosphorylation, whereas the infusion of ANP caused the expected murine VASP Ser-235 phosphorylation (Figure 18A). PGE1 infusion reduced the extent of myocardial tissue damage in the WT animals, yet we did not observe this effect in the *VASP*$^{-/-}$ animals. When using ANP to induce VASP Ser-235 phosphorylation, we also found a significant reduction of myocardial tissue injury in the WT animals, yet this was not present in *VASP*$^{-/-}$ animals (Figure 18B). The troponin I measurements confirmed the results of the tissue evaluation (Figure 18C). We then proceeded to identify possible presence of PNCs within the myocardial tissue of these animals, and found that in the animals treated with PGE1 or ANP only a small number of PNCs were present within myocardial tissue of WT animals (Figure 18E).

	WT	***VASP-/-***
anaesthesia *(mmHg)*	*95±2*	*93±2*
open chest *(mmHg)*	*83±2*	*88±2*
ischemia *(mmHg)*	*75±2*	*83±2*
reperfusion *(mmHG)*	*77±1*	*77±3*
reperfusion + PGE1 *(mmHG)*	*72±1*	*76±2*
reperfusion + ANP *(mmHG)*	*68±6*	*73±2*

Figure 17 – Hemodynamic values during experimental protocol.

Experimental animals were cannulated with a catheter into the carotid artery and blood pressure measurements determined during ischemia, reperfusion, injection of atrial natriurteic peptide (ANP) or prostanglandin E1 (PGE1) (data are mean ± SEM, n=6)

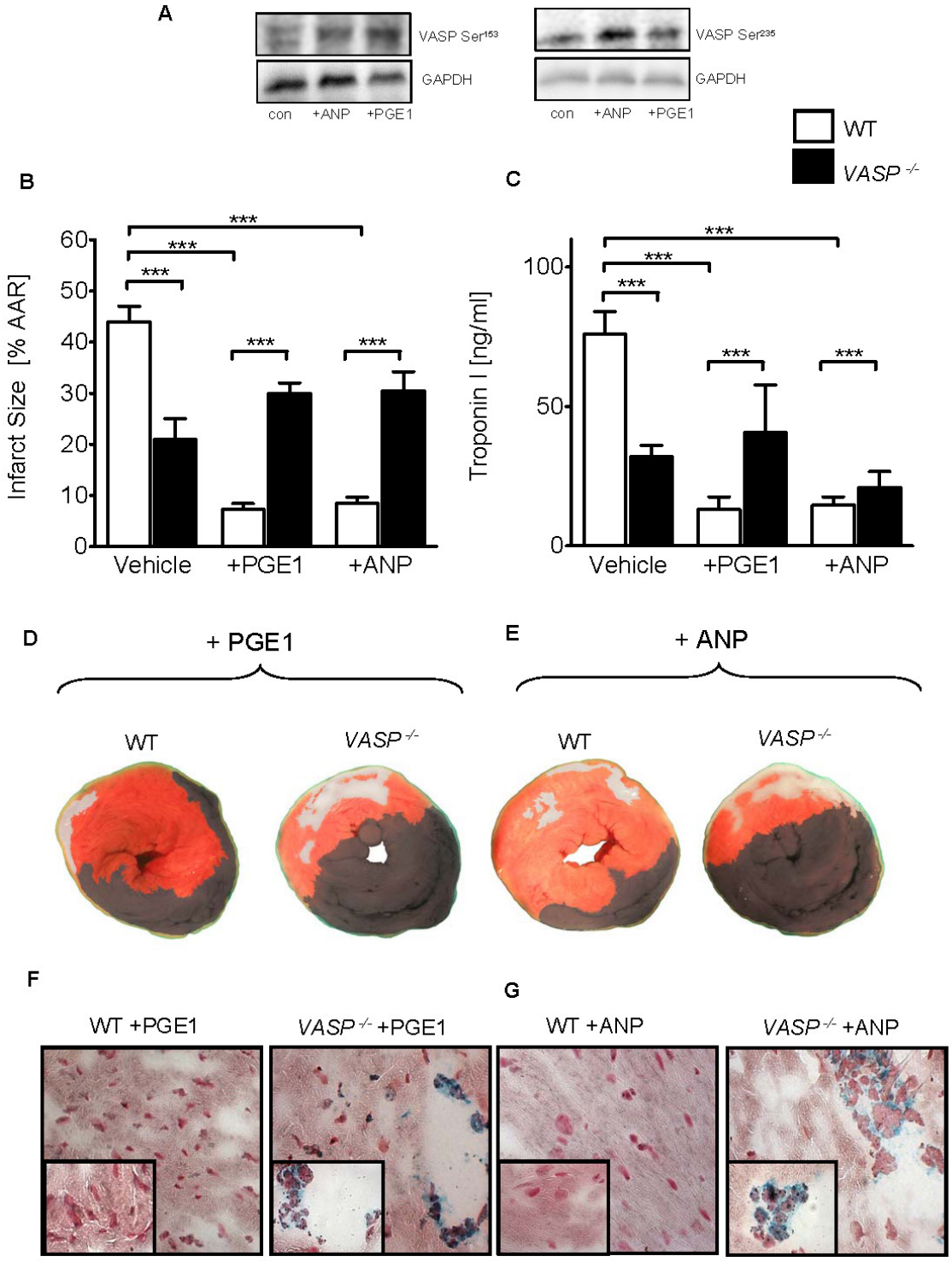

Figure 18 – VASP phosphorylation dampens myocardial IR injury.

A) Western Blots from whole blood samples from WT mice after injection with either prostaglandin E1 (PGE1) or atrial natriuretic peptide (ANP), showing VASP phosphorylation at murine VASP Ser-153 by PGE1 and at murine VASP Ser-235 by ANP **B)** Infarct size of WT and *VASP*$^{-/-}$ animals after 60 min of myocardial ischemia followed by 2 hours reperfusion with infusion of vehicle, PGE1 or ANP during reperfusion. The percentage of necrotic tissue to the

area at risk (AAR) is shown and **C)** Correlating serum troponin I values are depicted. **D)** Representative images of myocardial infarcts following PGE1 infusion or **E)** ANP infusion (blue/dark= retrograde Evan's blue staining; red and white= area at risk; white= infarcted tissue). **E**) Histological images of platelet-neutrophil complexes following PGE1 infusion or **G)** ANP infusion (PMNs = blue; platelets = black) in tissue sections of myocardial infarcts of all groups (data are shown as mean ± SEM, n=6, ***P < 0.001 as indicated, tissue sections magnification x400 and x1000, n=3, one representative of 3 individual experiments is demonstrated).

3.7 Phosphorylation of hematopoietic VASP reduces PNCs and myocardial IR injury.

Our previous experiments have demonstrated that hematopoietic derived VASP expression is of crucial importance for formation of PNCs during myocardial IR injury and dampens myocardial IR injury. We therefore continued to test the role of VASP phsophorylation in chimeric animals. For this purpose, we employed PGE1 and ANP in *VASP*$^{-/-}$→WT and WT→*VASP*$^{-/-}$ transplanted animals. Evaluation of the infarct size revealed that PGE1 significantly reduced myocardial tissue damage in the WT→*VASP*$^{-/-}$ transplanted animals but had no effect in the *VASP*$^{-/-}$→WT transplanted animals (Figure 19A and C). Similarly, ANP resulted in a significant reduction of myocardial tissue damage through VASP phosphorylation in the WT→*VASP*$^{-/-}$ transplanted animals, but had no effect in the WT→*VASP*$^{-/-}$ transplanted animals (Figure 19A and D). Troponin I measurement confirmed these findings (Figure 19B). In tissue sections we found a reduced presence of PNCs in the WT→*VASP*$^{-/-}$ transplanted animals compared to the *VASP*$^{-/-}$→WT transplanted animals following PGE1 or ANP infusion (Figure 19E and F).

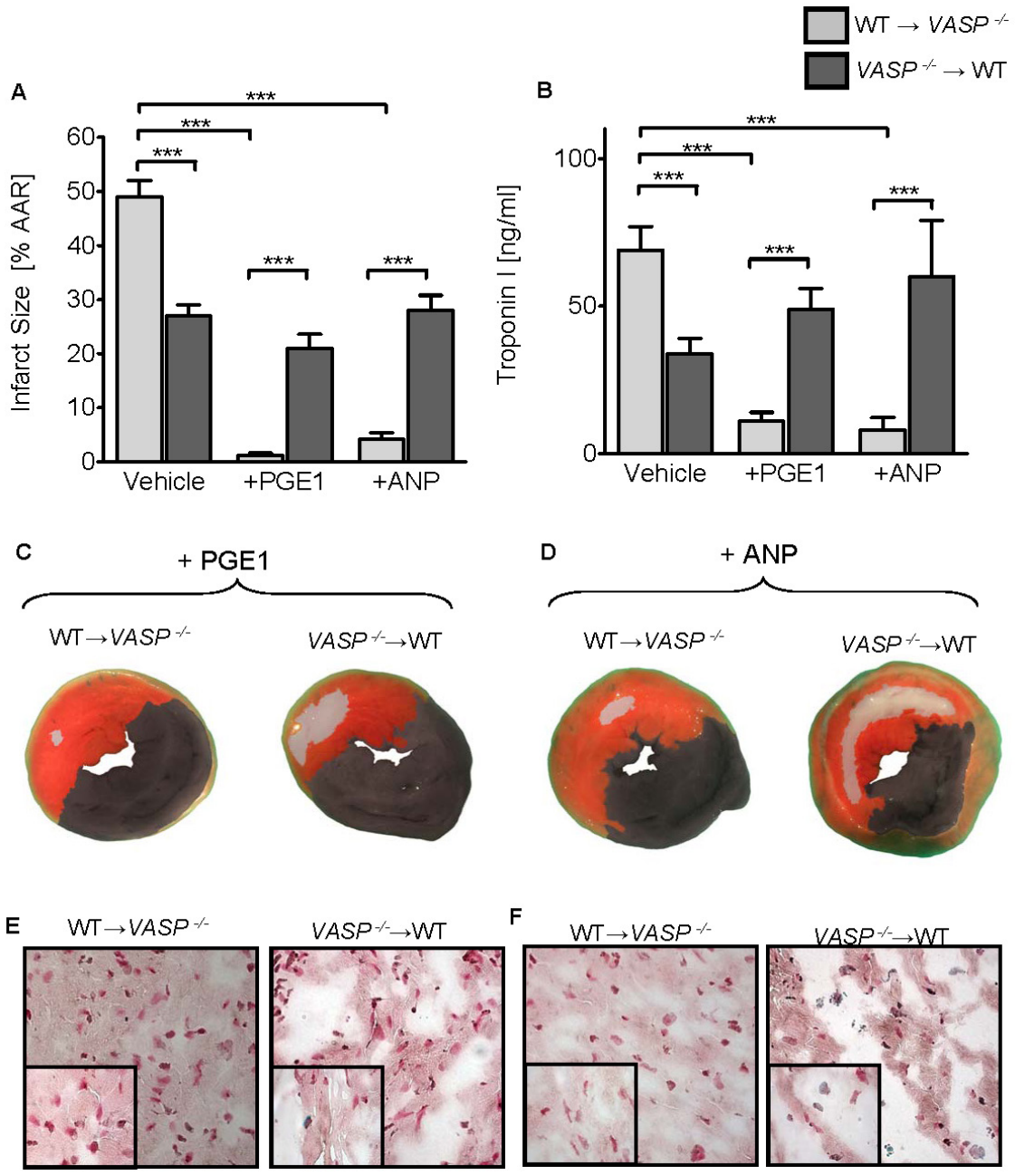

Figure 19 – Protective role of VASP phosphorylation is dependent on hematopoietic VASP expression.

A) Size of myocardial IR injury in chimeric animals (*VASP*$^{-/-}$→WT and WT→*VASP*$^{-/-}$) after 60 min of myocardial ischemia following 2 hours reperfusion and infusion of vehicle, PGE1 or ANP. The percentage of necrotic tissue to the area at risk (AAR) is calculated. **B)** Correlating serum troponin I values are depicted. **C)** Representative images of myocardial sections of infarcts from the experiment above after infusion of PGE1 or **D)** ANP (blue/dark, retrograde Evan's blue staining; red and white, area at risk; white, infarcted tissue). **E)** Platelet-neutrophil complexes (neutrophil = blue; platelet = black)) in sections of myocardial infarct tissue of

chimeric animals (*VASP*$^{-/-}$→WT and WT→*VASP*$^{-/-}$) after 60 min of myocardial ischemia following 2 hours reperfusion and infusion of PGE1 or **F)** ANP during reperfusion (data are shown as mean ± SEM, n=6, ****P* < 0.001 as indicated, tissue sections magnification x400 and x1000, n=3, one representative of 3 individual experiments is demonstrated).

4 Discussion

The extent of myocardial IR injury is influenced by neutrophils and platelets. Recent work has appreciated the importance of PNC formation during acute lung injury and has demonstrated that neutrophils facilitate the translocation of platelets into mucosal tissue.[66-67] The role of PNCs during myocardial IR injury however remains unclear, and a regulatory mechanism of PNC formation is not known. We have made clear that the cytoskeletal protein VASP significantly affects the formation of PNCs during myocardial IR injury. In initial studies we were able to demonstrate that VASP phosphorylation affects platelet translocation across endothelial cells. Studies employing *VASP*$^{-/-}$ and chimeric animals revealed that platelet derived VASP significantly influences the formation of PNCs, a process that could be prevented through VASP phosphorylation. This resulted in a significant reduction of myocardial IR injury. Therefore these studies define the functional impact of PNCs for myocardial tissue injury and identify VASP as a key regulatory protein for PNC formation.

In the study by Scotland et al. platelet-leukocyte interactions and PNC aggregate formation were reduced through C-type natriuretic peptide. This inhibition of PNC formation was accompanied by a reduced expression of P-selectin on the platelet surface.[83] C-type natriuretic peptide increases intracellular cGMP with subsequent phosphorylation of VASP on Ser-239.[84] An increase of cGMP within platelets is also mediated by nitric oxide (NO), a well-defined inhibitor of platelet activation and P-selectin expression, although stimulatory effects during the early phases of activation are discussed.[85-86] The phosphorylation of VASP in response to cGMP and cAMP has been described by several investigators.[87] A phosphorylation of VASP at Ser-157 reduces the affinity of the platelet fibrinogen receptor to bind fibrinogen and collagen, and therefore might well explain a reduced formation of PNCs.[78,87] In our study, we employed ANP to selectively induce phosphorylation of VASP at Ser-239 ([43]) and used PGE1 to induce VASP phosphorylation at the Ser-157 site in a cAMP dependent mechanism.[87-88] For firm adhesion between platelets and neutrophils

and the formation of PNCs, a link of the GPIIb/IIIa receptor on platelets and MAC-1 (CD11b/CD18) on neutrophils with their common ligand, fibrinogen, has to prevail.[89] Therefore the selective phosphorylation of VASP in platelets which we have demonstrated through ANP or PGE1 might well reduce the affinity of GPIIb/IIIa to fibrinogen and a firm adhesion to CD11b/CD18 on neutrophils. This results in a reduced formation of PNCs and as such dampens the extent of myocardial IR injury. This would at least in part provide further explanation of the clinically observed role of ANP and PGE1 to reduce the extent of myocardial IR injury if used during reperfusion.[90-91]

The functional importance of PNC formation for the extent of inflammatory tissue injury has been implicated previously. Kupatt et al. demonstrated that a reduction of the platelet-neutrophil interaction through c7E3Fab, a chimeric Fab fragment blocking GPIIb/IIIa resulted in improved postischemic recovery of external heart work measured as the ability of the myocardium to perform a defined pressure-volume work.[92] The crucial importance of the formation of PNCs for the extent of inflammatory tissue damage has been recognized in recent work by Zarbock et al. examining the role of the PNCs during acute lung injury.[66] Zarbock et al. were able to demonstrate that acid induced lung injury is aggravated by the formation of PNCs. An inhibition of this PNC formation resulted in a marked decrease of pulmonary injury and improved pulmonary function. This finding was corroborated by Looney et al. demonstrating that platelet depletion or aspirin pretreatment resulted in reduced transfusion related lung injury. However, in this study the interaction of neutrophils with platelets was not dependent on P-selectin.[93] Weissmüller et al. describe the importance of PNCs and the translocation of platelets through neutrophils across an epithelial cell barrier. The translocated platelets released ATP that induced the function of ectonucleotidases in the intestinal lumen.[67,94] This demonstrates that the translocated platelets are functionally intact. We showed that neutrophils facilitate transendothelial movement of platelets into the ischemic myocardial tissue. Furthermore, we demonstrate that this neutrophil facilitated platelet movement can be reduced through the phosphorylation of VASP, and this has

significant impact on myocardial tissue injury. This correlates well with the clinical strategy to reduced platelet activation during the reperfusion phase.[80] As confirmed through the depletion of platelets or neutrophils, we found no difference between the WT and the *VASP*$^{-/-}$ animals, which supports the fact that the formation of PNC is of crucial importance for the extent of myocardial tissue injury following IR.

5 Summary and Conclusions (Synopsis)

The results of our study are in line with previous investigations demonstrating the importance of PNCs for the extent of inflammatory tissue injury, and confirm that the reduction of PNC formation might be tissue protective. The regulatory role of VASP phosphorylation for the formation of PNC was identified *in-vitro* and transferred into *in-vivo* evidence. VASP phosphorylation on Ser-157 or Ser-239 resulted in reduced formation of PNC and dampened the extent of myocardial IR injury. This work therefore furthers the understanding of the mechanisms underlying the formation of PNC, supports the importance of PNC for the extent of IR injury and increases our understanding of the role of VASP during myocardial IR injury.

6 References

1. Halbrugge, M. & Walter, U. Purification of a vasodilator-regulated phosphoprotein from human platelets. *Eur J Biochem* **185**, 41-50 (1989).
2. Gambaryan, S., Hauser, W., Kobsar, A., Glazova, M. & Walter, U. Distribution, cellular localization, and postnatal development of VASP and Mena expression in mouse tissues. *Histochem Cell Biol* **116**, 535-543 (2001).
3. Wang, X., Pluznick, J.L., Settles, D.C. & Sansom, S.C. Association of VASP with TRPC4 in PKG-mediated inhibition of the store-operated calcium response in mesangial cells. *Am J Physiol Renal Physiol* **293**, F1768-1776 (2007).
4. Haffner, C.*, et al.* Molecular cloning, structural analysis and functional expression of the proline-rich focal adhesion and microfilament-associated protein VASP. *EMBO J* **14**, 19-27 (1995).
5. Sporbert, A.*, et al.* Phosphorylation of vasodilator-stimulated phosphoprotein: a consequence of nitric oxide- and cGMP-mediated signal transduction in brain capillary endothelial cells and astrocytes. *Brain Res Mol Brain Res* **67**, 258-266 (1999).
6. Ferron, F., Rebowski, G., Lee, S.H. & Dominguez, R. Structural basis for the recruitment of profilin-actin complexes during filament elongation by Ena/VASP. *EMBO J* **26**, 4597-4606 (2007).
7. Furman, C.*, et al.* Ena/VASP is required for endothelial barrier function in vivo. *J Cell Biol* **179**, 761-775 (2007).
8. Lum, H. & Malik, A.B. Regulation of vascular endothelial barrier function. *Am J Physiol* **267**, L223-241 (1994).
9. Malik, A. & Silfinger-Birnboim, A. Vascular Endothelial Barrier Function and Its Regulation. in *Biological Barriers to Protein Delivery* 231-267 (Andus, KL.; Raub, TL. , 1993).
10. Xiao, Z.L. & Sun, G.Y. [Research progress on regulation of vascular endothelial barrier function]. *Sheng Li Ke Xue Jin Zhan* **29**, 215-220 (1998).
11. Comerford, K.M., Lawrence, D.W., Synnestvedt, K., Levi, B.P. & Colgan, S.P. Role of vasodilator-stimulated phosphoprotein in PKA-induced changes in endothelial junctional permeability. *FASEB J* **16**, 583-585 (2002).
12. Henes, J.*, et al.* Inflammation-associated repression of vasodilator-stimulated phosphoprotein (VASP) reduces alveolar-capillary barrier function during acute lung injury. *FASEB J* (2009).
13. Barragan, P.*, et al.* Resistance to thienopyridines: clinical detection of coronary stent thrombosis by monitoring of vasodilator-stimulated phosphoprotein phosphorylation. *Catheter Cardiovasc Interv* **59**, 295-302 (2003).
14. Zarbock, A., Polanowska-Grabowska, R.K. & Ley, K. Platelet-neutrophil-interactions: linking hemostasis and inflammation. *Blood Rev* **21**, 99-111 (2007).

15. Geiger, J.*, et al.* Specific impairment of human platelet P2Y(AC) ADP receptor-mediated signaling by the antiplatelet drug clopidogrel. *Arterioscler Thromb Vasc Biol* **19**, 2007-2011 (1999).
16. Gurbel, P.A., Becker, R.C., Mann, K.G., Steinhubl, S.R. & Michelson, A.D. Platelet function monitoring in patients with coronary artery disease. *J Am Coll Cardiol* **50**, 1822-1834 (2007).
17. Ibanez, B., Vilhahur, G. & Badimon, J. Pharmacology of thienopyridines: rationale for dual pathway inhibition. *European Heart Journal Supplements* **8 (Supplement G)**, G3–G9 (2006).
18. Aleil, B.*, et al.* Flow cytometric analysis of intraplatelet VASP phosphorylation for the detection of clopidogrel resistance in patients with ischemic cardiovascular diseases. *J Thromb Haemost* **3**, 85-92 (2005).
19. Serebruany, V.L.*, et al.* Effects of clopidogrel and aspirin combination versus aspirin alone on platelet aggregation and major receptor expression in patients with heart failure: the Plavix Use for Treatment Of Congestive Heart Failure (PLUTO-CHF) trial. *Am Heart J* **146**, 713-720 (2003).
20. Angiolillo, D.J.*, et al.* Variability in individual responsiveness to clopidogrel: clinical implications, management, and future perspectives. *J Am Coll Cardiol* **49**, 1505-1516 (2007).
21. Frere, C.*, et al.* ADP-induced platelet aggregation and platelet reactivity index VASP are good predictive markers for clinical outcomes in non-ST elevation acute coronary syndrome. *Thromb Haemost* **98**, 838-843 (2007).
22. Schafer, A.*, et al.* ADP-induced platelet aggregation frequently fails to detect impaired clopidogrel-responsiveness in patients with coronary artery disease compared to a P2Y12-specific assay. *Thromb Haemost* **100**, 618-625 (2008).
23. Kwiatkowski, A.V., Gertler, F.B. & Loureiro, J.J. Function and regulation of Ena/VASP proteins. *Trends Cell Biol* **13**, 386-392 (2003).
24. Reinhard, M., Jarchau, T. & Walter, U. Actin-based motility: stop and go with Ena/VASP proteins. *Trends Biochem Sci* **26**, 243-249 (2001).
25. Kragtorp, K.A. & Miller, J.R. Regulation of somitogenesis by Ena/VASP proteins and FAK during Xenopus development. *Development* **133**, 685-695 (2006).
26. Zimmer, M.*, et al.* Cloning of the VASP (vasodilator-stimulated phosphoprotein) genes in human and mouse: structure, sequence, and chromosomal localization. *Genomics* **36**, 227-233 (1996).
27. Vanderzalm, P. & Garriga, G. Losing their minds: Mena/VASP/EVL triple knockout mice. *Dev Cell* **13**, 757-758 (2007).
28. Lambrechts, A.*, et al.* cAMP-dependent protein kinase phosphorylation of EVL, a Mena/VASP relative, regulates its interaction with actin and SH3 domains. *J Biol Chem* **275**, 36143-36151 (2000).
29. Howe, A.K., Hogan, B.P. & Juliano, R.L. Regulation of vasodilator-stimulated phosphoprotein phosphorylation and interaction with Abl by protein kinase A and cell adhesion. *J Biol Chem* **277**, 38121-38126 (2002).

30. Pasic, L., Kotova, T. & Schafer, D.A. Ena/VASP proteins capture actin filament barbed ends. *J Biol Chem* **283**, 9814-9819 (2008).
31. Benz, P.M.*, et al.* Cytoskeleton assembly at endothelial cell-cell contacts is regulated by alphaII-spectrin-VASP complexes. *J Cell Biol* **180**, 205-219 (2008).
32. Kuhnel, K.*, et al.* The VASP tetramerization domain is a right-handed coiled coil based on a 15-residue repeat. *Proc Natl Acad Sci U S A* **101**, 17027-17032 (2004).
33. Bachmann, C., Fischer, L., Walter, U. & Reinhard, M. The EVH2 domain of the vasodilator-stimulated phosphoprotein mediates tetramerization, F-actin binding, and actin bundle formation. *J Biol Chem* **274**, 23549-23557 (1999).
34. Zimmermann, J.*, et al.* Relaxation, equilibrium oligomerization, and molecular symmetry of the VASP (336-380) EVH2 tetramer. *Biochemistry* **41**, 11143-11151 (2002).
35. Holt, M.R., Critchley, D.R. & Brindle, N.P. The focal adhesion phosphoprotein, VASP. *Int J Biochem Cell Biol* **30**, 307-311 (1998).
36. Reinhard, M., Rudiger, M., Jockusch, B.M. & Walter, U. VASP interaction with vinculin: a recurring theme of interactions with proline-rich motifs. *FEBS Lett* **399**, 103-107 (1996).
37. Krause, M.*, et al.* Lamellipodin, an Ena/VASP ligand, is implicated in the regulation of lamellipodial dynamics. *Dev Cell* **7**, 571-583 (2004).
38. Moody, J.D.*, et al.* A zyxin head-tail interaction regulates zyxin-VASP complex formation. *Biochem Biophys Res Commun* **378**, 625-628 (2009).
39. Niebuhr, K.*, et al.* A novel proline-rich motif present in ActA of Listeria monocytogenes and cytoskeletal proteins is the ligand for the EVH1 domain, a protein module present in the Ena/VASP family. *EMBO J* **16**, 5433-5444 (1997).
40. Krause, M.*, et al.* Fyn-binding protein (Fyb)/SLP-76-associated protein (SLAP), Ena/vasodilator-stimulated phosphoprotein (VASP) proteins and the Arp2/3 complex link T cell receptor (TCR) signaling to the actin cytoskeleton. *J Cell Biol* **149**, 181-194 (2000).
41. Zhang, Y., Tu, Y., Gkretsi, V. & Wu, C. Migfilin interacts with vasodilator-stimulated phosphoprotein (VASP) and regulates VASP localization to cell-matrix adhesions and migration. *J Biol Chem* **281**, 12397-12407 (2006).
42. Boukhelifa, M., Parast, M.M., Bear, J.E., Gertler, F.B. & Otey, C.A. Palladin is a novel binding partner for Ena/VASP family members. *Cell Motil Cytoskeleton* **58**, 17-29 (2004).
43. Chen, H., Levine, Y.C., Golan, D.E., Michel, T. & Lin, A.J. Atrial natriuretic peptide-initiated cGMP pathways regulate vasodilator-stimulated phosphoprotein phosphorylation and angiogenesis in vascular endothelium. *J Biol Chem* **283**, 4439-4447 (2008).
44. Benz, P.M.*, et al.* Differential VASP phosphorylation controls remodeling of the actin cytoskeleton. *J Cell Sci* **122**, 3954-3965 (2009).

45. Blume, C.*, et al.* AMP-activated protein kinase impairs endothelial actin cytoskeleton assembly by phosphorylating vasodilator-stimulated phosphoprotein. *J Biol Chem* **282**, 4601-4612 (2007).
46. Abel, K., Mieskes, G. & Walter, U. Dephosphorylation of the focal adhesion protein VASP in vitro and in intact human platelets. *FEBS Lett* **370**, 184-188 (1995).
47. Beavo, J.A. & Brunton, L.L. Cyclic nucleotide research -- still expanding after half a century. *Nat Rev Mol Cell Biol* **3**, 710-718 (2002).
48. Ambudkar, I.S. Ca2+ signaling microdomains:platforms for the assembly and regulation of TRPC channels. *Trends Pharmacol Sci* **27**, 25-32 (2006).
49. O'Neil, R.G. VASP: a TRPC4-associated phosphoprotein that mediates PKG-induced inhibition of store-operated calcium influx. *Am J Physiol Renal Physiol* **293**, F1766-1767 (2007).
50. Dimmeler, S.*, et al.* Activation of nitric oxide synthase in endothelial cells by Akt-dependent phosphorylation. *Nature* **399**, 601-605 (1999).
51. Cudmore, M.*, et al.* VEGF-E activates endothelial nitric oxide synthase to induce angiogenesis via cGMP and PKG-independent pathways. *Biochem Biophys Res Commun* **345**, 1275-1282 (2006).
52. Miggin, S.M. & Kinsella, B.T. Investigation of the mechanisms of G protein: effector coupling by the human and mouse prostacyclin receptors. Identification of critical species-dependent differences. *J Biol Chem* **277**, 27053-27064 (2002).
53. Ewert, R., Schaper, C., Halank, M., Glaser, S. & Opitz, C.F. Inhalative iloprost - pharmacology and clinical application. *Expert Opin Pharmacother* **10**, 2195-2207 (2009).
54. Reny, J.L. & Cabane, J. [Buerger's disease or thromboangiitis obliterans]. *Rev Med Interne* **19**, 34-43 (1998).
55. Poredos, P. Possibilities for clinical use of prostacyclin in vascular disease. *Pflugers Arch* **440**, R137-138 (2000).
56. Landolfi, R., Di Gennaro, L. & Falanga, A. Thrombosis in myeloproliferative disorders: pathogenetic facts and speculation. *Leukemia* **22**, 2020-2028 (2008).
57. Yellon, D.M. & Hausenloy, D.J. Myocardial reperfusion injury. *N Engl J Med* **357**, 1121-1135 (2007).
58. Sisley, A.C., Desai, T., Harig, J.M. & Gewertz, B.L. Neutrophil depletion attenuates human intestinal reperfusion injury. *J Surg Res* **57**, 192-196 (1994).
59. Singbartl, K., Green, S.A. & Ley, K. Blocking P-selectin protects from ischemia/reperfusion-induced acute renal failure. *Faseb J* **14**, 48-54 (2000).
60. Nachman, R.L. & Weksler, B. The platelet as an inflammatory cell. *Ann N Y Acad Sci* **201**, 131-137 (1972).
61. Weyrich, A.S. & Zimmerman, G.A. Platelets: signaling cells in the immune continuum. *Trends Immunol* **25**, 489-495 (2004).
62. Xu, Y.*, et al.* Activated platelets contribute importantly to myocardial reperfusion injury. *Am J Physiol Heart Circ Physiol* **290**, H692-699 (2006).

63. Zimmerman, G.A. Two by two: the pairings of P-selectin and P-selectin glycoprotein ligand 1. *Proc Natl Acad Sci U S A* **98**, 10023-10024 (2001).
64. Ley, K., Laudanna, C., Cybulsky, M.I. & Nourshargh, S. Getting to the site of inflammation: the leukocyte adhesion cascade updated. *Nat Rev Immunol* **7**, 678-689 (2007).
65. Gawaz, M., Langer, H. & May, A.E. Platelets in inflammation and atherogenesis. *J Clin Invest* **115**, 3378-3384 (2005).
66. Zarbock, A., Singbartl, K. & Ley, K. Complete reversal of acid-induced acute lung injury by blocking of platelet-neutrophil aggregation. *J Clin Invest* **116**, 3211-3219 (2006).
67. Weissmuller, T.*, et al.* PMNs facilitate translocation of platelets across human and mouse epithelium and together alter fluid homeostasis via epithelial cell-expressed ecto-NTPDases. *J Clin Invest* (2008).
68. Pasquet, J.M., Noury, M. & Nurden, A.T. Evidence that the platelet integrin alphaIIb beta3 is regulated by the integrin-linked kinase, ILK, in a PI3-kinase dependent pathway. *Thromb Haemost* **88**, 115-122 (2002).
69. Altmann, C.*, et al.* Sphingosylphosphorylcholine, a naturally occurring lipid mediator, inhibits human platelet function. *Br J Pharmacol* **138**, 435-444 (2003).
70. Bennett, J.S., Zigmond, S., Vilaire, G., Cunningham, M.E. & Bednar, B. The platelet cytoskeleton regulates the affinity of the integrin alpha(IIb)beta(3) for fibrinogen. *J Biol Chem* **274**, 25301-25307 (1999).
71. Anderson, S.I., Behrendt, B., Machesky, L.M., Insall, R.H. & Nash, G.B. Linked regulation of motility and integrin function in activated migrating neutrophils revealed by interference in remodelling of the cytoskeleton. *Cell Motil Cytoskeleton* **54**, 135-146 (2003).
72. Pasic, L., Kotova, T.I. & Schafer, D.A. Ena/VASP proteins capture actin filament barbed ends. *J Biol Chem* (2008).
73. Rosenberger, P.*, et al.* Hypoxia-inducible factor-dependent induction of netrin-1 dampens inflammation caused by hypoxia. *Nat Immunol* **10**, 195-202 (2009).
74. Henes, J.*, et al.* Inflammation-associated repression of vasodilator-stimulated phosphoprotein (VASP) reduces alveolar-capillary barrier function during acute lung injury. *Faseb J* **23**, 4244-4255 (2009).
75. Hauser, W.*, et al.* Megakaryocyte hyperplasia and enhanced agonist-induced platelet activation in vasodilator-stimulated phosphoprotein knockout mice. *Proc Natl Acad Sci U S A* **96**, 8120-8125 (1999).
76. Eckle, T.*, et al.* Systematic evaluation of a novel model for cardiac ischemic preconditioning in mice. *Am J Physiol Heart Circ Physiol* (2006).
77. Fishbein, M.C.*, et al.* Early phase acute myocardial infarct size quantification: validation of the triphenyl tetrazolium chloride tissue enzyme staining technique. *Am Heart J* **101**, 593-600 (1981).
78. Horstrup, K.*, et al.* Phosphorylation of focal adhesion vasodilator-stimulated phosphoprotein at Ser157 in intact human platelets correlates with fibrinogen receptor inhibition. *Eur J Biochem* **225**, 21-27 (1994).

79. Jensen, B.O., Selheim, F., Doskeland, S.O., Gear, A.R. & Holmsen, H. Protein kinase A mediates inhibition of the thrombin-induced platelet shape change by nitric oxide. *Blood* **104**, 2775-2782 (2004).
80. Sabatine, M.S.*, et al.* Addition of clopidogrel to aspirin and fibrinolytic therapy for myocardial infarction with ST-segment elevation. *N Engl J Med* **352**, 1179-1189 (2005).
81. Bhatt, D.L.*, et al.* Intravenous platelet blockade with cangrelor during PCI. *N Engl J Med* **361**, 2330-2341 (2009).
82. Bellemain-Appaix, A.*, et al.* Slow response to clopidogrel predicts low response. *J Am Coll Cardiol* **55**, 815-822.
83. Scotland, R.S.*, et al.* C-type natriuretic peptide inhibits leukocyte recruitment and platelet-leukocyte interactions via suppression of P-selectin expression. *Proc Natl Acad Sci U S A* **102**, 14452-14457 (2005).
84. Kim, D.*, et al.* Angiotensin II increases phosphodiesterase 5A expression in vascular smooth muscle cells: a mechanism by which angiotensin II antagonizes cGMP signaling. *J Mol Cell Cardiol* **38**, 175-184 (2005).
85. Radomski, M.W., Palmer, R.M. & Moncada, S. An L-arginine/nitric oxide pathway present in human platelets regulates aggregation. *Proc Natl Acad Sci U S A* **87**, 5193-5197 (1990).
86. Li, Z., Zhang, G., Feil, R., Han, J. & Du, X. Sequential activation of p38 and ERK pathways by cGMP-dependent protein kinase leading to activation of the platelet integrin alphaIIb beta3. *Blood* **107**, 965-972 (2006).
87. Nolte, C., Eigenthaler, M., Horstrup, K., Honig-Liedl, P. & Walter, U. Synergistic phosphorylation of the focal adhesion-associated vasodilator-stimulated phosphoprotein in intact human platelets in response to cGMP- and cAMP-elevating platelet inhibitors. *Biochem Pharmacol* **48**, 1569-1575 (1994).
88. Comerford, K.M., Lawrence, D.W., Synnestvedt, K., Levi, B.P. & Colgan, S.P. Role of vasodilator-stimulated phosphoprotein in protein kinase A-induced changes in endothelial junctional permeability. *Faseb J* (2002).
89. Weber, C. & Springer, T.A. Neutrophil accumulation on activated, surface-adherent platelets in flow is mediated by interaction of Mac-1 with fibrinogen bound to alphaIIbbeta3 and stimulated by platelet-activating factor. *J Clin Invest* **100**, 2085-2093 (1997).
90. Kawamura, T., Nara, N., Kadosaki, M., Inada, K. & Endo, S. Prostaglandin E1 reduces myocardial reperfusion injury by inhibiting proinflammatory cytokines production during cardiac surgery. *Crit Care Med* **28**, 2201-2208 (2000).
91. Kitakaze, M.*, et al.* Human atrial natriuretic peptide and nicorandil as adjuncts to reperfusion treatment for acute myocardial infarction (J-WIND): two randomised trials. *Lancet* **370**, 1483-1493 (2007).
92. Kupatt, C.*, et al.* c7E3Fab reduces postischemic leukocyte-thrombocyte interaction mediated by fibrinogen. Implications for myocardial reperfusion injury. *Arterioscler Thromb Vasc Biol* **20**, 2226-2232 (2000).
93. Looney, M.R.*, et al.* Platelet depletion and aspirin treatment protect mice in a two-event model of transfusion-related acute lung injury. *J Clin Invest* **119**, 3450-3461 (2009).

94. Kohler, D*., et al.* CD39/ectonucleoside triphosphate diphosphohydrolase 1 provides myocardial protection during cardiac ischemia/reperfusion injury. *Circulation* **116**, 1784-1794 (2007).

7 Appendix

7.1 Statement of Contribution

Conception of this thesis, acquisition, analysis and interpretation of data and manuscript writing have been accomplished in cooperation with and under the supervision of Prof. Dr. Peter Rosenberger and Dr. rer. nat. David Köhler. Additionally some of the experiments of this work were not exclusively produced by the author but in collaboration with Marion Faigle and David Köhler (Flourescence activated cell sorting, transendothelial migration assey), Stephanie Zug (Immunhistochemistry assay), Rainer Lehmann (troponin assay) and David Köhler (Animal experiments). It is to note that parts of this study have presently been submitted to be published beyond this doctoral thesis.

Add:

Publication note: June 2011

Kohler, D., *et al.* Phosphorylation of vasodilator-stimulated phosphoprotein prevents platelet-neutrophil complex formation and dampens myocardial ischemia-reperfusion injury. *Circulation* **123**, 2579-2590 (2011).

7.2 Acknowledgements

I thank Prof. Dr. Peter Rosenberger for giving me the opportunity to write this thesis and giving me an insight view of medical research functioning.

Special sincere thanks to my supervising tutors Dr. rer. nat. David Köhler and Marion Faigle for always being there, when I needed professional advice or support. Without your organisation skills I would not have been able to finish this thesis!

Additionally I would like to thank:

- Alice Mager, Stephanie Zug, Stefanie Laucher, Michaela Hoch-Gutbrod, Irene Vollmer and Stefanie Stark for assisting my first steps of experimental research, helping out with all kinds of experiments, answering my questions patiently and giving their best to preserve a good working climate despite all conflicts.
- Julio Morote Garcia for being a good example that working hard pays off, for being a good tutor to Daniel and for always being supportive.
- Christof Zanke for all kind of technical assistance.
- Lukas Kleine for his helping hand throughout all research experiments, for spreading good mood and sharing good laughs.
- Dorothee Boos for cross-reading the manuscript.

Furthermore, I would like to thank my parents for their financial and moral support throughout my years of study. Without you I wouldn’t stand where I am today!

I would like to extend my heartfelt gratitude to my beloved family and closest friends for their great confidence and honesty. My warmest embrace to you all.

Last but not least my most cordial thanks to Daniel Napiwotzky. I love you for being at my side anytime I need you, for encouraging me to proceed, when I have any doubts, for your patience, inspiration and guidance, and for everything words can’t describe!